Design of a Resistance-Based High Temperature Liquid Metal Flow Meter

by

Logan Vawter

Submitted to the
Department of Mechanical Engineering
in Partial Fulfillment of the Requirements for the Degree of

Bachelor of Science in Mechanical Engineering

at the

Massachusetts Institute of Technology

May, 2022

Signature of Author:

_____

Department of Mechanical Engineering
May 6, 2022

Certified by:

_____

Asegun Henry
Associate Professor of Mechanical Engineering
Thesis Supervisor

Accepted by:

_____

Kenneth Kamrin
Associate Professor of Mechanical Engineering
Undergraduate Officer

Design of a Resistance-Based High Temperature Liquid Metal Flow Meter

by

Logan Vawter

Submitted to the Department of Mechanical Engineering
on May 6, 2022 in Partial Fulfillment of the
Requirements for the Degree of
Bachelor of Science in Mechanical Engineering

ABSTRACT

Flow rate is a parameter that is vital to measure in high temperature pumped liquid metal systems, yet traditional flow meters are unable to perform at these extreme conditions. As a part of the Atomic Simulation & Energy (ASE) Research Group here at MIT, this research seeks to develop a flow meter able to measure the 1200 ºC pumped liquid tin in their methane pyrolysis system. This paper presents a summary of a literature review of methods for measuring liquid metal flow rate. The most viable method allows flow rate to be determined by a height measurement through Torricelli's law. While liquid metal surface height can be measured in a variety of ways, this paper explores the use of a resistant-based measurement. After reviewing existing designs, an original simple rod design and temperature-insensitive rod-sheath design are presented. A working prototype of the rod-sheath design is detailed and discussed with an experimental procedure as well as considerations recommended for continued work on this inquiry.

Thesis Supervisor: Dr. Asegun Henry
Title: Associate Professor of Mechanical Engineering

Acknowledgements

Special thanks to Professor Henry, Michael Bichnevicius, Mehdi Pishahang, Collin Kelsall, and Quinn Chappelle for their support and guidance on this thesis.

Table of Contents

Abstract 3
Acknowledgements 4
Table of Contents 5
List of Figures 6
List of Tables 7
1. Introduction 8
1.1 Motivation 8
1.2 System and Device Specifications 8
2. Liquid Metal Flow Rate Measurement Review 9
3. Liquid Metal Height Measurement Review 11
4. Resistance-Based Height Measurement Review 16
4.1 I-tube 16
4.2 J-Tube 18
5. Flow Meter Tank Design Considerations 19
6. Resistance-Based Height Measurement Design 21
6.1 Simple Rod Design 21
6.2 Rod-Sheath Design 25
7. Resistance-Based Height Measurement Prototype and Experiments 31
7.1 Tin Experiment 34
8. Future Work 35
9. Summary 37

List of Figures

Figure 1: Point Contact Level Indicators (left) Insulated Type, (right) High Resistance Type 12
Figure 2: Differential Pressure Level Indicators (left) Dual Sensor Type, (right) Bubbler Type 13
Figure 3: Float Level Indicators (left) Surface Type, (right) Displacer Type 14
Figure 4: Induction Level Indicator 14
Figure 5: Electrical Capacitance Level Indicator 15
Figure 6: Resistance I-Tube (left) Top Mounted, (right) Bottom Mounted 16
Figure 7: Briggs I-probe (left) Design (right) Equivalent Circuit 17
Figure 8: CEA J-tube (left) Design, (right) Equivalent Circuit 18
Figure 9: Oak Ridge J-tube (left) Design, (right) Equivalent Circuit 19
Figure 10: Surface height (as a percentage of maximum height) as a function of flow rate 20
Figure 11: Simple Rod (a) Design, (b) Equivalent Circuit 21
Figure 12: Resistivity of CFC and Tin 22
Figure 13: Simple Rod Design Resistances 23
Figure 14: Simple Rod Design Calibration Curve 23
Figure 15: Simple Rod Design Temperature Dependence 24
Figure 16: Rod-sheath (a) Design, (b) equivalent circuit 25
Figure 17: Resistivity of CFC, Tin, and Tungsten 26
Figure 18: Rod-Sheath Design Resistances 27
Figure 19: Rod-Sheath Voltage Divider Circuit 27
Figure 20: Rod-Sheath Design Voltage Divider Output 28
Figure 21: Rod-Sheath Design Two Branch Circuit 29
Figure 22: Rod-Sheath Design Branch Currents 29
Figure 23: Rod-Sheath Design Two Branch Output 30
Figure 24: Rod-Sheath Design Calibration Curve 31
Figure 25: Rod-Sheath Height Measurement Prototype 32
Figure 26: Prototype Measured Resistances 34
Figure 27: Prototype Experiment Output 35

List of Tables

Table 1: Prototype Rod and Sheath Expected Resistance 33
Table 2: Conducting Fluids 33
Table 3: Metal Melting Points 36

1. Introduction

1.1 Motivation

Pumped liquid metals have potential applications in energy technology, especially at high temperatures (>1000 ºC). Measuring flow rate is necessary in these systems, but proves difficult to accomplish, especially at the laboratory scale. Commercially available flow meters are not designed to function at such high temperatures and would melt or quickly corrode. Therefore, it is imperative to explore and apply novel techniques to flow meters so more energy technology and energy-based solutions can be explored in the laboratory process.

Directed by Dr. Asegun Henry, the Atomic Simulation & Energy (henceforth to be referred to as ASE) Research Group at the Massachusetts Institute of Technology (MIT) is exploring applications of pumped liquid metals, specifically tin. Their thermal grid energy storage (TEGS) project offers a solution to the energy storage needs associated with decarbonization and the switch to renewable energy sources. The system converts excess electricity into heat stored in graphite blocks. Heat can then be transferred to a thermophotovoltaic heat engine, converting the energy back into electricity as needed. Pumped liquid tin is vital for this system as it is used to transfer heat from the refractory heating element to the graphite storage blocks, and from the storage blocks to the TPV heat engine.

Another application of pumped liquid tin being explored by the group is in the production of hydrogen. Molecular hydrogen is championed as a green alternative fuel source that would allow for the decarbonization of the transportation sector, but the grim reality is that the vast majority of current hydrogen production releases CO_2 as a byproduct. The dirty process, known as steam-methane reformation, is so prevalent because it is cheaper and more efficient than currently investigated renewable approaches, predominantly due to their fundamentally higher reaction enthalpies. However, one method being investigated by the ASE Research Group has a lower reaction enthalpy: Methane Pyrolysis. Also known as Methane Cracking, the method uses heat to decompose methane, CH_4, into solid carbon black and H_2. The method requires high temperatures and high heat flux, which can be delivered by a liquid tin bubble column. Complete pyrolysis is inhibited when carbon accumulates, clogging the reactor. This can be avoided by continually pumping the tin to remove the carbon. The adoption of this method worldwide would lower global greenhouse gas emissions, allow hydrogen to be sustainably scaled as a green fuel, and produce valuable carbon black for industrial and commercial applications. [1]

While experiments can be conducted using pumped liquid metal without the need for a flow rate measurement, determining a quantity for flow rate characterizes the capabilities of the system. Without a flow meter, it is difficult to verify system performance and compute other parameters that rely on flow rate. Therefore, this research is crucial to progress the ongoing research at the ASE Research Group and will impact the field of energy technology beyond.

1.2 System and Device Specifications

While a high temperature liquid flow meter could be used in a wide variety of applications, the scope of this thesis focuses on meeting the needs of the ASE Research Group, specifically for the Methane Pyrolysis project. The flow meter will therefore be designed to measure the flow rate of pumped molten tin in the hydrogen production system, which ranges from 0 to 1 L/min, and will be brought to the flow meter by a 1/8" inner diameter tube. At room temperatures, tin is relatively unreactive and does not corrode or rust, however, the temperature of the tin in the system is around 1200 ºC. At temperatures this high, tin reacts easily with oxygen forming tin oxide (SnO_2), therefore the gas environment is primarily argon, and the oxygen partial pressure is kept less than $1*10^{-15}$ ppm. The flow meter should have a 95% confidence interval uncertainty no greater than 100mL/min. As space is constrained within the system, the flow meter should occupy no more than 216 cubic inches. The flow meter should be reusable and capable of providing continuous measurement over its use. Finally, the measuring area should be fully enclosed and covered in thermal insulation. [2]

2. Liquid Metal Flow Rate Measurement Review

[Measuring velocity in high-temperature liquid metals: a review]

First, we conducted a literature review, exploring a wide variety of ways to measure flow rate. A summary of each method is given below. The ability of each method to meet the specifications outlined in section 1.2 is evaluated, and their limitations are discussed.

One potential way to get data on flow rate is to measure surface velocity using photographic methods. By taking video of the flow surface, the distance traveled by reference objects between frames can be used to determine surface velocities. These reference objects can take many forms. An object separate from the fluid, such as a glass bead, will be swept by the flow along the surface and have a rigid form for detection in each frame. Alternatively, there may be visual variations in the fluid itself, such as bright spots caused by surface slag or dark striations in the flow. Due to the extreme temperatures of our system and the need for thermal insulation, a visual inspection of the tin will not be possible whether manually or by remote viewing through a camera. [3]

Another method uses reaction probes to measure the force exerted by the flowing liquid. These probes are characterized by a body such as a disk, plate, or sphere submerged in the fluid paired with a measuring device. A body subjected to fluid flow experiences an average drag force D directly related to the fluid velocity V

$$D = 0.5\rho V^2 A C_D \tag{1}$$

where ρ is the density of the fluid, A is the flow-normal cross-sectional area, and C_D is the drag coefficient. Because fluid density is a function of temperature, this method would require temperature calibration. In one procedure, a strain gauge attached to the submerged body measures the drag it experiences. Alternative procedures include a spring-loaded rod paired with a linear voltage differential transformer or the use of a load cell. Unfortunately, it would be very difficult to transmit the force experienced by the submerged body across a distance far enough for the measuring device to avoid experiencing errors or even complete failure due to the extreme temperatures. Therefore, a different method, lacking this sizable issue, is preferable for the research's needs. [3]

Another method involves introducing a small amount of radioactive tracer at one point in the flow and taking samples periodically some distance downstream. The tracer chosen must have a decay that is effectively negligible over the experiment duration. The concentration of the tracer measured at the sampling location is a function of time, velocity, and diffusivity. By measuring tracer concentration over time, curve fitting can be used to reveal velocity and diffusivity. This technique is cumbersome as it only measures average velocity over a large area and a finite length of time. [3]

Another method makes use of electromagnetic effects to measure velocity because liquid metal is a conducting fluid. Applying a stationary magnetic field across the flow will induce a voltage difference across a nearby pair of electrodes. The electromagnetic properties of the system are directly related to the total flow velocity V through Ohm's law for a moving conductor

$$\boldsymbol{J} = \sigma(\boldsymbol{E} + \boldsymbol{V} \times \boldsymbol{B}) \tag{2}$$

where J is the current density, σ is the electrical conductivity, E is the electric field, and B is the magnetic field. This method requires extensive and difficult calibration, and external electric or magnetic fields can interfere. This method is also inadequate for low flow rates, because the magnetic field produced would be too weak. Furthermore, permanent magnets are temperature sensitive: the strength of the magnetic field slowly decreases as temperature rises before dropping abruptly near the Curie temperature. Because of this phenomenon, this method is better suited for liquid metals below 720ºC operating at high flow rates. [3]

Another method estimates velocity by measuring the rate of mass loss of a submerged body. Through dissolution and melting studies, calibration curves can be created that correlate liquid metal velocity with mass loss. In the case of dissolution, the submerged body should be a different material than the fluid, such as an iron rod in a liquid aluminum flow or a carbon rod in a low-carbon steel flow. Mass

loss can be determined by weighing the rods or measuring the change in diameter. In the case of melting, the submerged body should be the same material as the fluid such as an aluminum sphere in a liquid aluminum flow or a steel sphere in a liquid steel flow. Experimentally, sphere melting time and liquid metal velocity have been found to have a decreasing linear relationship. The mass loss method works up to very high liquid metal temperatures but can only estimate an average velocity over a large area and over an extended period of time. The need to replace the mass after each measurement rules this method out. [3]

Another option is to use a fiber-optic velocity sensor. The fiber-optic sensor consists of a glass pointer sealed into the end of a thin-walled glass cone. The pointer's free end is placed between four light guides, two of which are connected optically to a light source, with the other two being connected to photocells. The blackened free end partially blocks the two beams in its initial position. When the sensor is placed in a fluid flow, the pointer deflects proportional to velocity, changing the amount of light reaching the photocells. Thus, once calibrated, two components of the velocity can be measured by the electrical signals from the photocells. This method is limited, however, by its reliance on fluid momentum, making accurate measurements nearly impossible at lower flow rates. [3]

The final method explored relies on the behavior of fluid flowing out an orifice at the bottom of a tank due to hydrostatic pressure. Taking a point 1 at the orifice and a point 2 on the free surface (and assuming that the points lie on a streamline, the fluid has constant density, the flow is steady, and there is no friction) we can apply Bernoulli's Equation

$$(h_2 - h_1) + \left(\frac{P_2 - P_1}{\rho g}\right) + \left(\frac{v_2^2 - v_1^2}{2g}\right) = 0 \tag{3}$$

where h is height, P is pressure, ρ is fluid density, g is gravitational acceleration, and v is velocity. The difference between h_2 and h_1 is the height h of the liquid surface above the orifice. Each point is at atmospheric pressure. When the orifice is much smaller than the cross-sectional area of the tank, v_2 is negligible. Plugging in these conditions we get a relationship known as Torricelli's law.

$$h = \left(\frac{v_1^2}{2g}\right) \tag{4}$$

$$v_1 = \sqrt{2gh} \tag{5}$$

The fluid velocity leaving the orifice matches the velocity that a water droplet would acquire after falling freely a height h, where gravitational potential energy is converted into kinetic energy. Fluid velocity v is related to volumetric flow rate

$$\dot{V} = A_o v \tag{6}$$

where A_o is the cross-sectional area of the orifice. Starting from an empty tank, if liquid metal enters at a constant flow rate, the surface height of the fluid in the tank will rise. As the surface height increases, so will the outlet flow rate. Once the flow rate in equals the flow rate out, the system will be in equilibrium and a steady-state height and flow rate will be reached for that specific flow rate according to equations 7 and 8.

$$h = \left(\frac{\left(\dot{V}/A_o\right)^2}{2g}\right) \tag{7}$$

$$\dot{V} = A_o\sqrt{2gh} \tag{8}$$

If the inlet flowrate decreases, the outlet flow rate will momentarily be larger, causing the liquid surface height to drop until reaching a new equilibrium. The nature of this method means there is a time delay between a change in system flow rate and the liquid level reaching the new corresponding steady state height, as the tank must drain or fill. It should be noted that using this method, experimental results tend to not quite agree with theoretical models, as real tanks drain more slowly than Torricelli's law predicts. This discrepancy may be attributed to surface tension effects at the outlet hole that cause the liquid to drain slower than expected. The discrepancy may also be attributed to the formation of a vena contracta due to streamline convergence which causes the contracted, or effective, orifice area to be smaller than the actual area. These discrepancies can be accounted for by the introduction of a discharge coefficient μ as seen in equation 9.

$$\dot{V}_{actual} = \mu A\sqrt{2gh} \tag{9}$$

Furthermore, operation of such a flow meter does not need to rely on theoretical models. By allowing the liquid to naturally drain completely from full in a calibration drain test, the experimental results can be used to relate flow rate at each height for that specific tank. At the lowest flow rates, however, discrepancies are more difficult to account for. When the height of the fluid falls beneath a few millimeters above the outlet orifice, experimental results show that the tank does not drain properly with the fluid dripping out of the outlet rather than flowing. Overall, this method is very promising for measuring liquid metal flow rate, especially when compared to the previously mentioned methods. Its ingenuity lies in the fact that it replaces the difficult to measure, dynamic variable of flow rate, with a simple, static measurement of height. While other flow rate measurement methods break down at extreme temperatures, Torricelli's law holds true for all non-viscous liquids regardless of temperature. This method comes with a great deal of versatility as liquid metal surface height can be measured in a variety of ways. [4][5][6][7]

3. Liquid Metal Height Measurement Review

One potential method, previously explored under the supervision of Dr. Asegun Henry, determines the liquid height by a weight measurement. Subtracting the weight of the empty tank from the total measurement determines the total mass of fluid in the tank. Knowing the fluid's density and the tank's geometry, specifically its cross-sectional area, the height of the liquid can be inferred. In this method, mass flow rate can replace fluid velocity or volumetric flow rate. This method is calibrated through a drain test, where the resulting drain curve relates the fluid mass to time. Mass flow rate is represented by the slope of this drain curve, allowing the expected mass flow rate to be known for every measured mass. In theory, this relationship is represented by equation 10

$$\dot{m} = A_t\sqrt{\frac{2g\rho m}{A_o}} \tag{10}$$

where $\dot{m}$ is mass flow rate, A_t is the cross-section area of the tank, ρ is the density of the fluid, m is the mass of the fluid, and A_o is the cross-section area of the orifice. In practice, the calibration curve resulting from the drain test diverges from the expected relationship in equation 10. Therefore, the calibration data must be used to determine a suitable discharge coefficient. While advantageous that all measurements are taken externally, a major challenge for this method lies in the measurement technique. Experimental observations have shown that the signal of the weight scale tends to drift with changes in temperature. For a fixed mass, scale readings changed by 10% when ambient temperatures were increased by 20ºC. Nearly all scales measure weight using a load cell made up of strain gauges. Temperature changes cause modulus of elasticity changes and thermal expansion, which induce new strains and affect the electrical resistance of the gauge. Attempts to reduce thermal contact of the tank with the scale require bulky structures and attempts to control the temperature of the scale through cooling still create temperature swings due to

transient cooling profiles. Due to these limitations, other height measurement techniques must be explored. [6] [7] [8] [9]

One of the simplest ways to measure liquid metal height is the point contact method, as seen in figure 1. This method uses an electrical contact probe fed through an insulated bushing at the top of the tank and held at a specific height. When the fluid level remains below the height of the probe, the electrical circuit is closed. When the fluid level reaches the probe's height, the liquid metal acts as the other contact of a switch and closes the circuit. In this way, a binary 'On/Off' measurement determines whether the fluid surface is above or below the reference height. While this method is not continuous, liquid height can be measured at a range of discrete point values by using multiple probes of varying lengths. Alternatively, resistive metal thimbles can replace contact probes and insulating bushings. In this setup, the circuit will show a low resistance when the liquid metal makes contact with the thimble and a high resistance when the liquid level is low, and the thimble is alone. Improper or incomplete wetting of liquid metal on the probe, thimble, and vessel walls will cause errors in indication when the liquid metal surface reaches the reference height. The tendency of liquid metal vapor to condense on the insulating bushing will cause the circuit to be closed even while the liquid level is low. The lack of continuous indication is a major drawback for this method. [9] [10]

Within the point contact method, thermal contact probes offer an alternative to electrical probes. A thermocouple placed at a reference height will read the temperature of the cover gas when the liquid level is low and the temperature of the metal once it makes contact. For accurate results, this method relies on the temperatures of the liquid metal and cover gas to be meaningfully different. At temperatures above 700ºC, radiative heat transfer begins to dominate causing the assumption of distinct temperatures to be invalid. [9] [11]

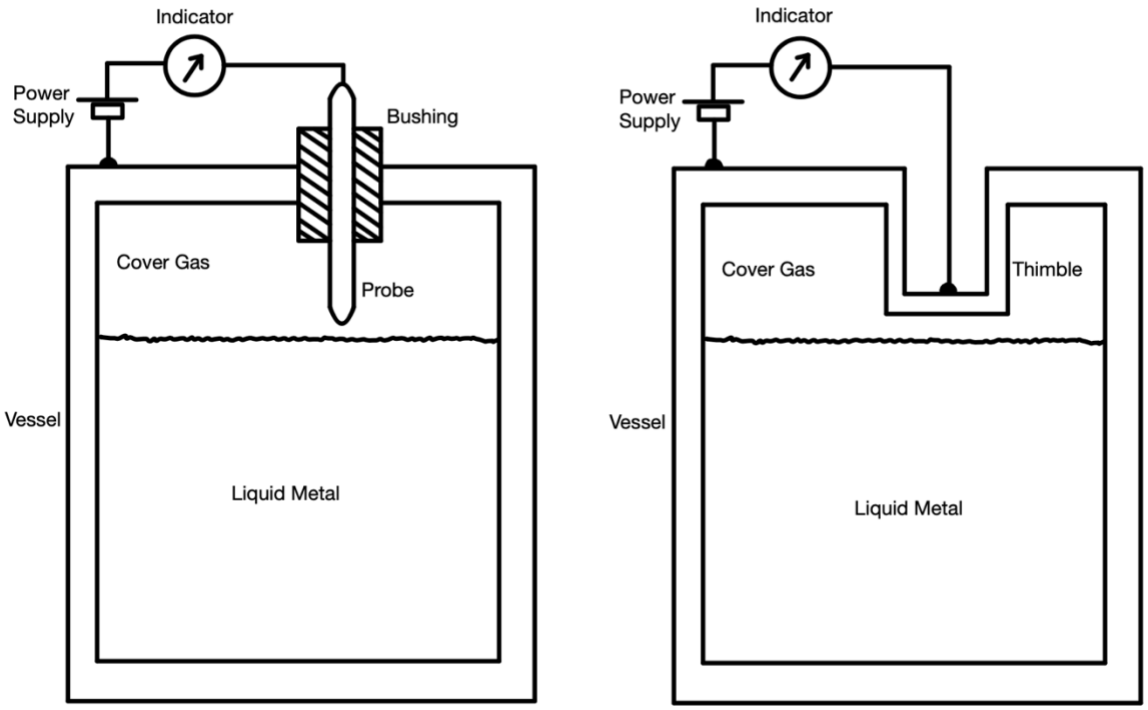

Figure 1: Point Contact Level Indicators (left) Insulated Type, (right) High Resistance Type

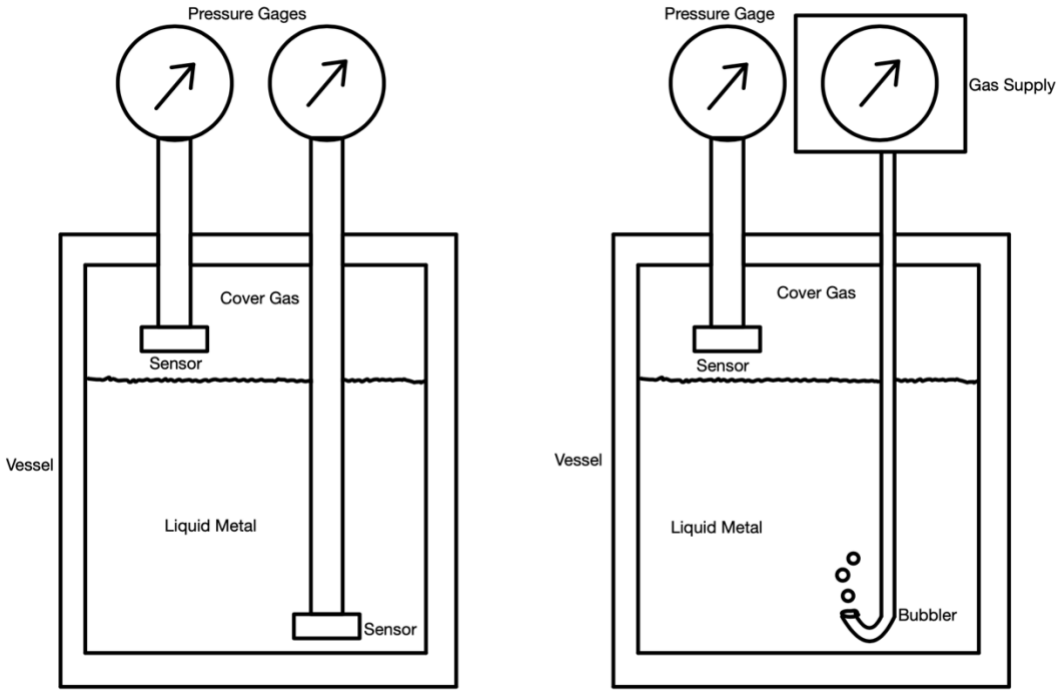

Figure 2: Differential Pressure Level Indicators (left) Dual Sensor Type, (right) Bubbler Type

Pressure operated devices offer a method for determining liquid surface height by measuring the hydrostatic pressure at the bottom of the tank as seen in figure 2. A typical setup requires two pressure transducers, offering a differential pressure measurement. One sensor near the top of the tank measures the pressure of the cover gas, while the other sensor at the bottom of the tank measures the pressure of the cover gas added to the hydrostatic head of the fluid. The conversion from pressure to liquid height is dependent on the density of the fluid. Because liquid metal density varies with temperature, compensation is required for accurate results. The shortcoming of this method lies in the need to immerse a pressure sensor in liquid metal, as it is likely to corrode and even melt. The bubbler technique offers a way to measure the pressure at the bottom of the tank by way of an external pressure measurement. The setup involves a gas supply connected to a tube whose end is immersed at the bottom of the tank. Gas will begin bubbling from the end of the tube once the gas supply pressure overcomes the pressure at the bottom of the tank. Therefore, the difference between the gas supply pressure that produces bubbling, and the cover gas pressure reveals the hydrostatic head of the fluid. [9] [10]

The float method uses buoyancy to measure liquid height as seen in figure 3. The simplest setup requires a pivot arm attached to a small surface float. As the liquid level rises, buoyancy keeps the float at the surface, causing the arm to raise. A device indicating position such as a displacement transducer is actuated by the arm, measuring the height of the liquid surface. The need for moving parts, specifically the pivot arm and displacement transducer, is the main drawback of this method, as vapor and oxide will deposit at the joints, disrupting the motion and the accuracy of the measurement. An alternative replaces the surface float with a larger and longer displacement float. This cylindrical float is suspended from the top of the tank so as the liquid level rises around the float, the buoyancy force increases by the weight of the liquid it displaces following Archimedes' principle. This causes a change in the effective weight of the float that is proportional to the liquid surface level, which can be measured by a force transducer, typically a positioning sensor device paired with a torsion bar or leaf spring. This method is temperature dependent as the

buoyancy force depends on liquid metal density which varies with temperature. The method is also prone to errors in the presence of swirling currents or other fluid motion. Furthermore, oxide and vapor deposition can disrupt the effectiveness of the force transducer. [9] [10]

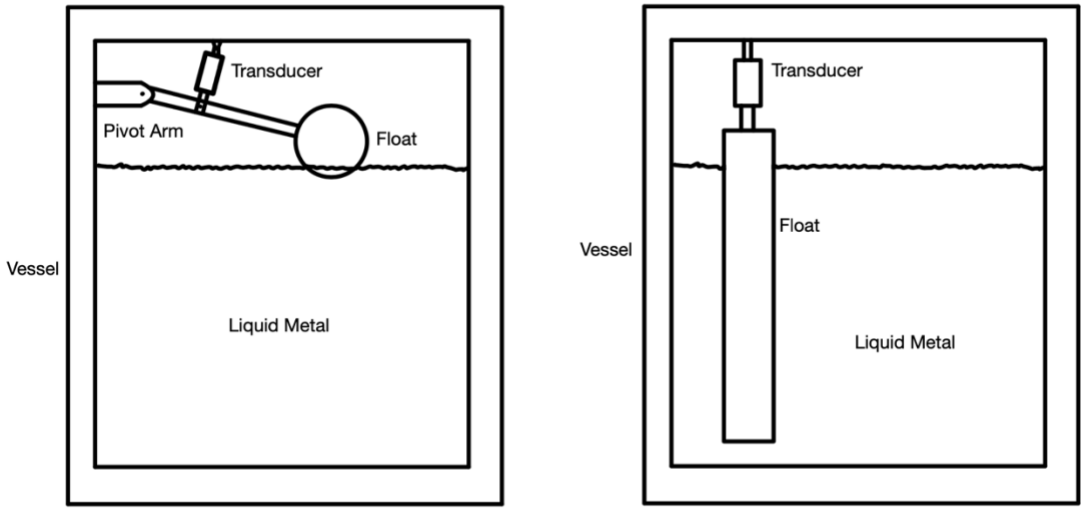

Figure 3: Float Level Indicators (left) Surface Type, (right) Displacer Type

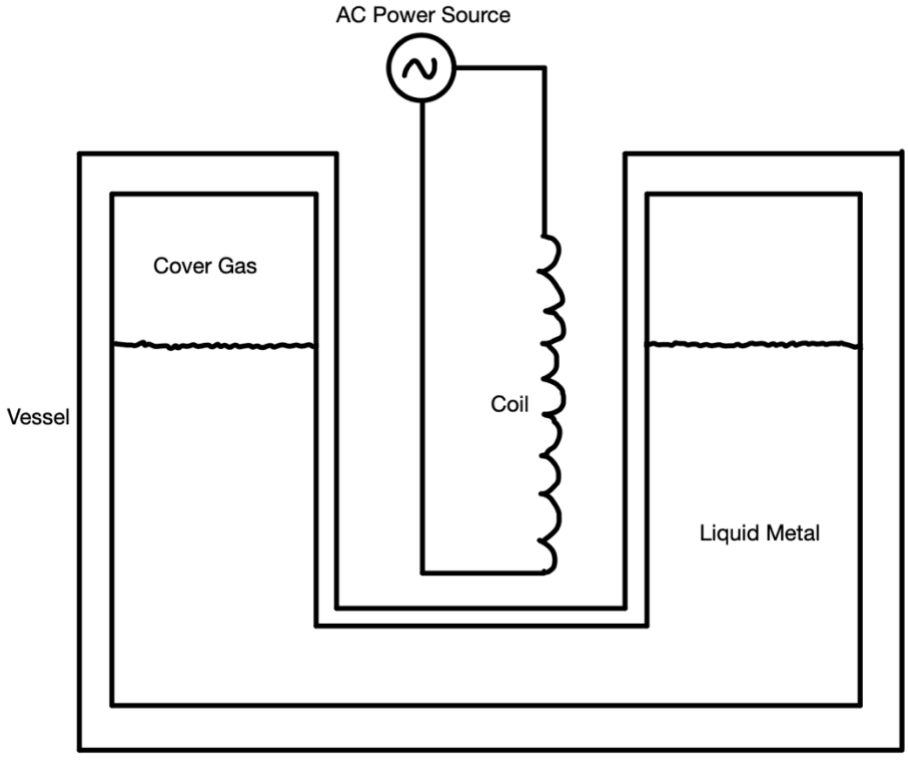

Figure 4: Induction Level Indicator

Inductive probes make use of the electrical properties of liquid metals to measure liquid height as seen in figure 4. The simplest setup requires a coil inserted into a thimble that drops down through the tank. The induction principle allows a current to be induced in the thimble and the surrounding liquid metal when the coil receives an alternating current. This induction consumes power at a rate proportional to the liquid height around the thimble, offering continuous level indication. The current induced in the thimble and surrounding liquid is a function of their resistances which are dependent on temperature. The temperature sensitivity of the resistivity of the coil can be significantly reduced by the use of low temperature coefficient wire. Furthermore, the dependence on coil resistance can be removed by the use of the mutual inductance between coupled coils. Either way, however, temperature dependence in the resistivity of the thimble and liquid metal remains. This temperature sensitivity can be compensated for by a reference coil placed in the thimble but above the maximum height of the liquid level. The maximum reliable temperature, typically around 800ºF, is limited by the coil. The use of magnesia insulation and high temperature stainless steel wire may allow temperatures to approach 2000ºF during operation. [9]

Capacitance probes are another option based in the electrical properties of liquid metal as seen in figure 5. The sensor in this method is a metal rod coated with insulation, such as alumina, that is inserted down into the tank, parallel to the vessel wall. When liquid level is low, the vessel wall and metal rod act as parallel capacitance plates with the insulation and cover gas acting as the dielectric. Where the liquid level rises around the rod, the liquid and metal rod act as capacitance plates with just the insulation acting as the dielectric. In this way, the capacitance value increases as the liquid surface height increases, and the change can be measured continuously by a capacitance meter, typically a capacitance bridge. It is important to note that this method is sensitive to temperature fluctuations. [9] [10]

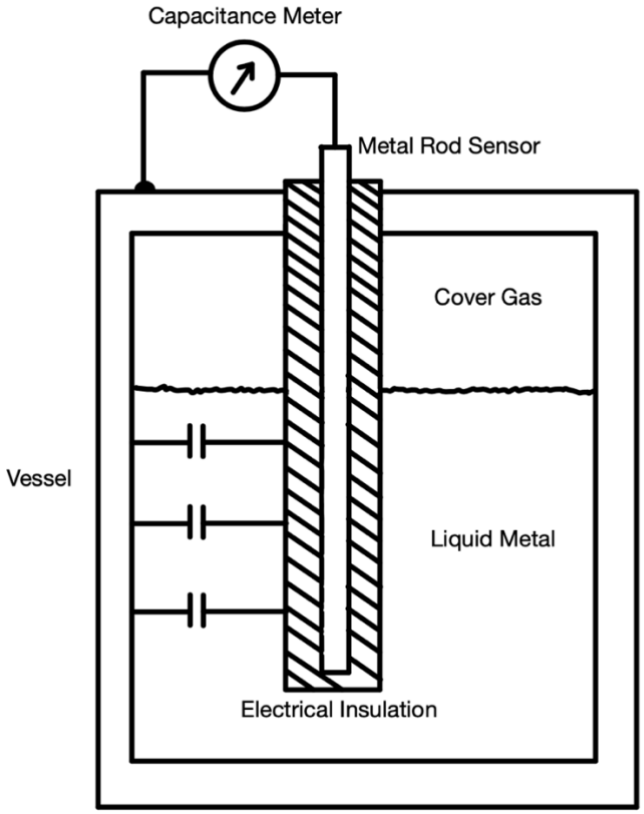

Figure 5: Electrical Capacitance Level Indicator

The final method explored connects liquid level to a simple resistance measurement. This method relies on a probe, typically a rod or tube, placed vertically inside the tank to act as a resistor. Because liquid metal is a conductor with low resistivity, as the fluid level rises, the resistance of the section of the probe covered is negated by the much lower shunt resistance provided by the liquid metal. The measurement of the probe's resistance therefore decreases linearly with fluid surface height. Because the liquid metal becomes a part of the circuit, this method relies on complete surface wetting in order to ensure electrical connection, which can be assured at temperatures greater than 800 ºF. Below this threshold, the surface condition of the material heavily affects wetting. Furthermore, the resistance of the probe is sensitive to temperature fluctuations. [10]

4. Resistance-Based Height Measurement Review

The 1950s and 1960s were a time of great progress in the field of atomic energy. This progress came with a lot of work on experimental fast-neutron nuclear reactors which used sodium-potassium alloy (NaK) as coolant. The need to measure the liquid level in coolant pump bowls led to the invention of a multitude of resistance-based level indicators.

4.1 I-Tube

The first type of level indicator, known as an I-tube, has a straight tube protrude vertically into the tank, with wires connected to the closed end. A common setup has the tank wall act as ground, one wire has a voltage input, and the other wire is used to measure output voltage as seen in figure 6. Mounting the tube from the top of the tank offers accessibility and simpler fabrication, but comes with reduced sensitivity and non-linear voltage output when the tank wall acts in parallel with the probe. On the other hand, while mounting the tube from the bottom of the vessel offers the best linearity and sensitivity, it requires proper sealing making it less accessible and problematic to fabricate. Both mounting directions rely on the same operating principle of probe resistance decreasing with liquid level. [9]

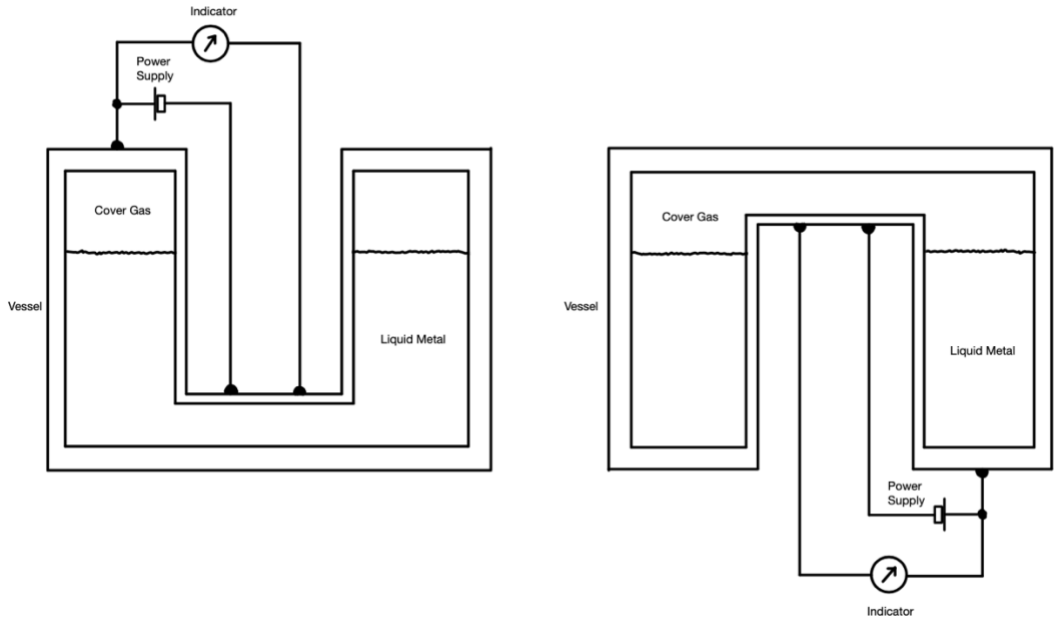

Figure 6: Resistance I-Tube (left) Top Mounted, (right) Bottom Mounted

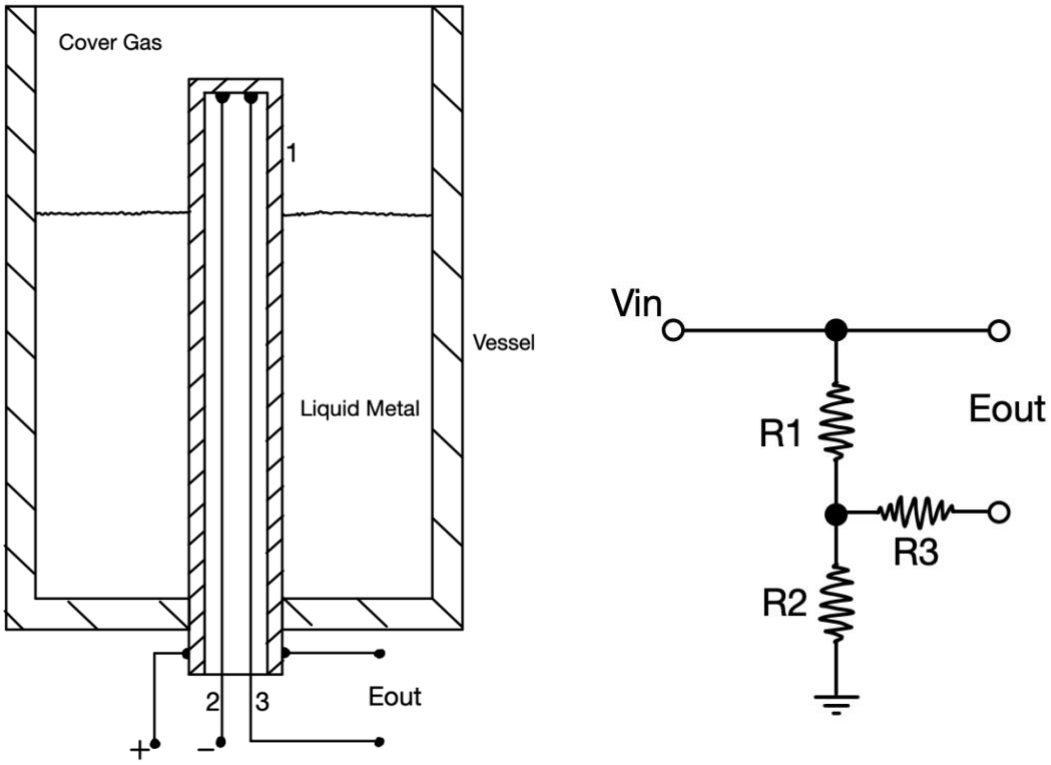

Figure 7: Briggs I-probe (left) Design (right) Equivalent Circuit

A 1968 patent filed by Norman H Briggs, as seen in figure 7, expands upon the I-tube design. His simplest "I" probe is a tubular sheath made from Inconel or stainless steel within which is appropriate insulation and two wires connected to the closed end. The probe is bottom mounted and sealed permanently by fusion. A DC source causes current to flow into the bottom of the sheath, with one of the wires being connected to ground. The other wire is used to measure the voltage drop across the length of the sheath, a measurement inversely proportional to liquid level. This setup acts as a voltage divider where the recorded Eout is determined by the resistances of the sheath and wire as seen by equation 11

$$E_{out} = V_{in}\left(\frac{R_1}{R_1+R_2}\right) \approx V_{in}\left(\frac{R_1}{R_2}\right) \; when \; R_1 \ll R_2 \tag{11}$$

where R_1 is the sheath resistance and R_2 is the wire resistance. By using the same material for the sheath and wires, temperature changes keep the ratio of the respective resistances constant, allowing the device to be temperature insensitive. Measurement errors may persist, however, due to the generation of thermoelectric voltages (EMF's). Thermal EMF's are generated because of temperature gradients at junctions of different conductors, in this case, the sheath and the liquid or the sheath and the vessel wall. These thermal EMF's add to the output signal by a voltage amount V

$$V = Q(T_1 - T_2) \tag{12}$$

where Q is the Seebeck Coefficient of material 2 with respect to material 1, and $T_1 - T_2$ is the temperature difference between them. The thermal EMF's can be eliminated by placing an identical "I" probe close to the active one. In the twin-"I" probe setup, the inactive probe generates an equal but opposite thermoelectric voltage. [12] [13]

4.2. J-Tube

The J-tube design achieves the sensitivity and linearity offered by the orientation of the bottom mounted I-tube without the need for permanent sealing. This probe is bent into a J shape so that it can be mounted from the top of the tank while the shorter vertical section does the sensing. This strange configuration achieves the best of both the top and bottom mounted I-tube designs, but sacrifices fabricability. Lead wires are particularly difficult to connect to the closed end of the tube, and shorts between the lead wires and tube walls lead to probe failure. Furthermore, special care must be taken in the fabrication of the J joints in order to avoid leaks. The bottom of the J to the top of the sensing tube covers the range of continuous level values this probe can measure. [9]

By 1966, the French Atomic Energy Commission (CEA) used a J-tube, as seen in figure 8, for level indication in their first sodium-cooled experimental fast nuclear reactor known as Rapsodie. The design was a simple 4-wire J-tube made of stainless steel consisting of a DC input and an output that measured the potential difference defined by the resistance of the sensing tube. The wires and tube were electrically isolated and sealed at the top. A large compensation resistor was placed in series with the third wire to reduce temperature dependence and to simplify the output ratio. However, the compensation was insufficient as the temperature of the resistor did not match the temperature of the tube. This was solved by later winding the resistor around the support tube. The measured output voltage is determined by the resistances of the sensing tube and compensation resistor

$$E_{out} \approx V_{in}\left(\frac{R_t}{R_c}\right) when\ R_c \gg R_t,\ R_{wires} \tag{13}$$

where R_t is the sensing tube resistance and R_c is the compensating resistance. [14]

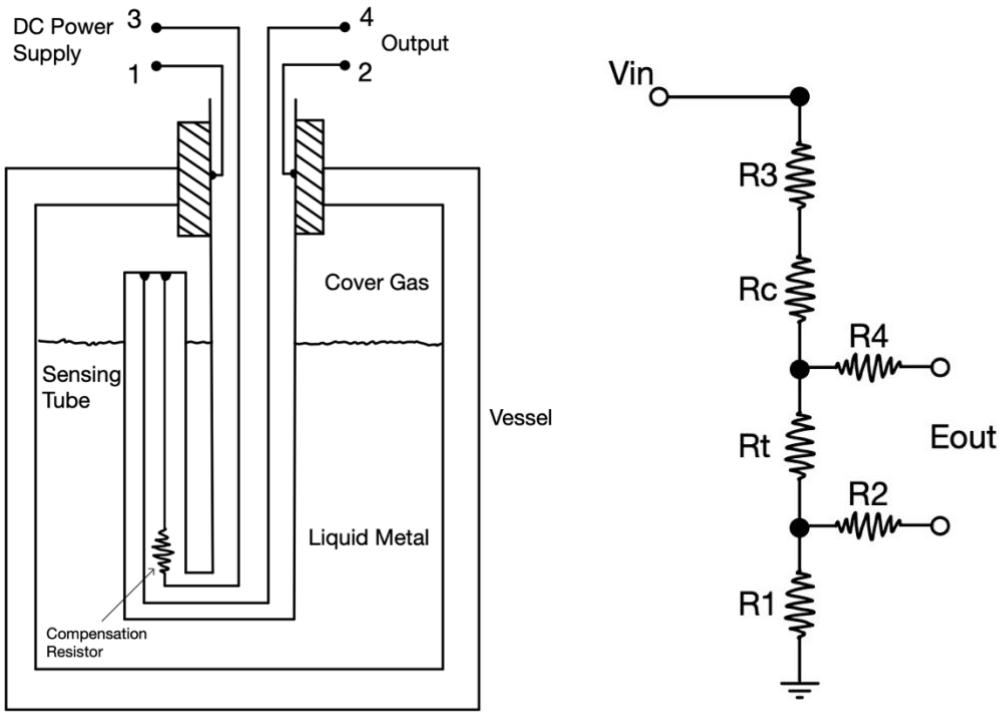

Figure 8: CEA J-tube (left) Design, (right) Equivalent Circuit

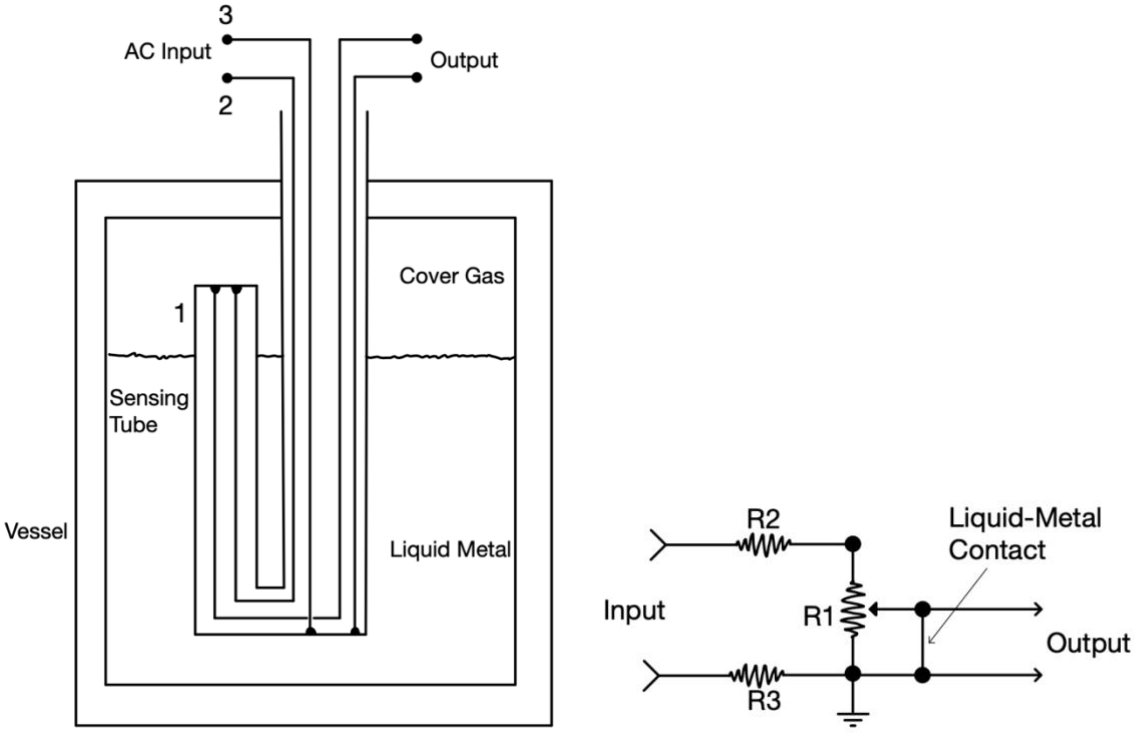

Figure 9: Oak Ridge J-tube (left) Design, (right) Equivalent Circuit

By 1960, another kind of J-tube, as seen in figure 9, was developed at Oak Ridge National Laboratory for use in the bowl of their NaK pumps. The probe is made entirely of Inconel, with magnesium oxide insulation inside. This 4-wire J-tube design had two AC inputs, recorded the voltage drop across the sensing tube, and relied on the tank walls to act as earth ground in the circuit. The input current leads act as compensating resistances so must be made of the same material as the sensing tube. The output voltage is related to these resistances

$$E_{out} = V_{in}\frac{R_1}{R_1+R_2+R_3} \approx V_{in}\frac{R_1}{R_2+R_3}\ when\ R_1 \ll R_2 + R_3 \tag{14}$$

where R_1 is the sensing tube resistance and R_2 and R_3 are the current lead resistances. The resulting experimental calibration curve is quite linear, except for the end effects caused by the termination of the current and voltage wires. In practice, some temperature dependence remains as the temperature dependence of the resistivity of Inconel wire and pipe may be slightly different, and they may not be in thermal equilibrium. [15]

5. Flow Meter Tank Design Considerations

The flow meter tank should be made from a high temperature material such as DS-4 graphite. It should have a flat bottom so it can be free-standing and a lid such that it can be fully enclosed. The probes and the inlet pipe should come down through the lid which is either made of insulating material or contains insulating bushings. The tank should be heavily insulated in order to thermally isolate it from sensitive measuring devices. To prevent splashing, the inlet pipe can be inserted deep into the tank cavity. On the side of the tank there should be an outlet orifice near the bottom and an overflow outlet included near the top so the tank can drain quickly if flow rates exceed expectations. These outlets could be made by tube and ferrule connections; however, these may experience leaks at extreme conditions. [6] Alternatively,

outlets could be machined as sharp-edged holes directly in the tank side and protected by tubular splash guards. The distance between the outlet orifice and the overflow hole determines the range of heights the flow meter can measure. Because the maximum flow rate we want to measure is 1.0 L/min, or 1.67e-5 m^3/s, we can relate the outlet orifice diameter to the maximum liquid surface height above the orifice as seen in equation 15.

$$D_o = \frac{0.00219}{\sqrt[4]{h_{max}}}\ m \tag{15}$$

For the selection of the maximum liquid surface height above the orifice, it is important to find the right balance. The taller that height, the more resolution the flow meter will offer, but smaller heights allow for a more compact design with quicker response time to equilibrium changes. In order to achieve useful measurement results, the response time (within 95% of final value) for the liquid to reach a new steady-state height due to a change in flow rate should not exceed 60 seconds. This response time is related to the cross-sectional area and height of the tank. Interestingly, for two tanks with equal volumes, the taller and skinnier one will drain faster than the shorter and wider one. Furthermore, the tank will take longer to fill than it will to drain, with each incremental liquid height increase towards the final value taking longer than the last.

It should be noted that because Torricelli's law is not a linear relationship, evenly spaced increments in flow rate do not correspond to evenly spaced increments in height. In fact, low flow rates correspond to heights squeezed more closely together than higher flow rates as seen by figure 10.

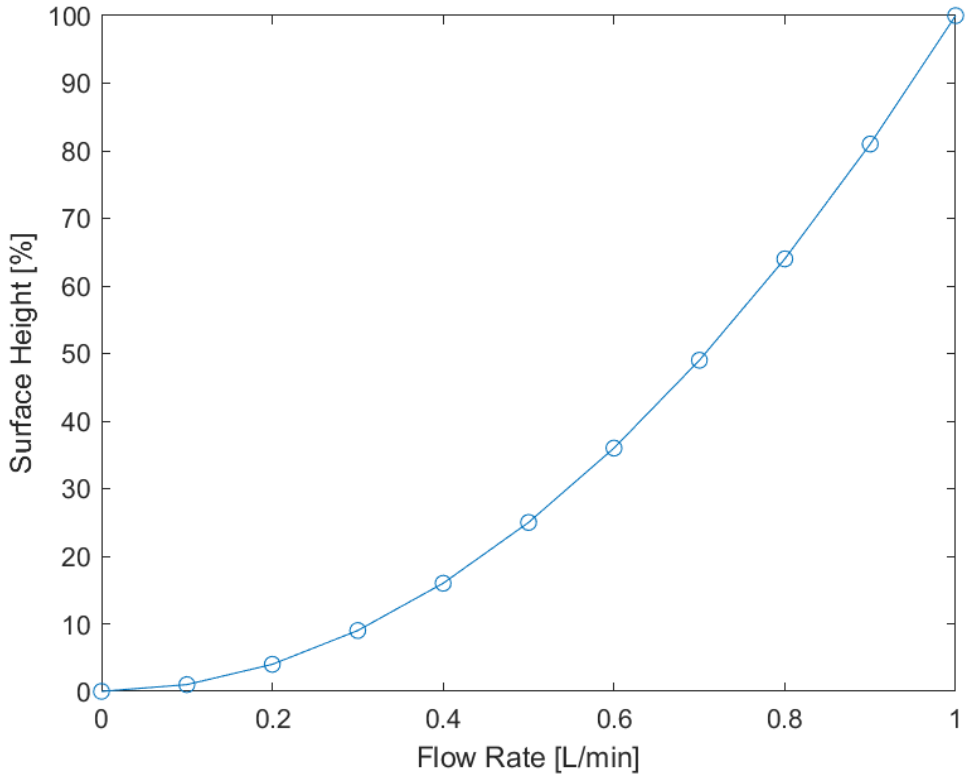

Figure 10: Surface height (as a percentage of maximum height) as a function of flow rate

6. Resistance-Based Height Measurement Design

6.1 Simple Rod Design

The simplest circuit setup for a resistance-based height measurement would be to have just one variable resistor immersed in the liquid metal. In order to avoid any complicated fabrication or sealing issues, this can be accomplished by inserting two rods from the top of the tank and measuring the resistance across them. Carbon fiber composite (CM-147 or PC-70) was selected as the rod material for its ability to withstand high temperatures, and its large resistivity when compared to tin. In order to support the vertical rods, the tank can be modified with blind holes drilled into the bottom. The rods should be threaded so they can be fastened to low resistivity threaded rods such as tungsten. This allows the circuit to be taken out of the insulated environment without adding too much extra resistance, that way the recorder can be operated at tolerable temperatures while still reading an accurate resistance for the relevant CFC rod length.

Nominal choices put the CFC rod geometry at ¼" diameter and 12” length, with 1” of space between them. We will set the maximum surface height to 6” or 0.1524, which according to equation 15 means the orifice diameter should be 0.0035m. The design and its equivalent circuit are shown in figure 11.

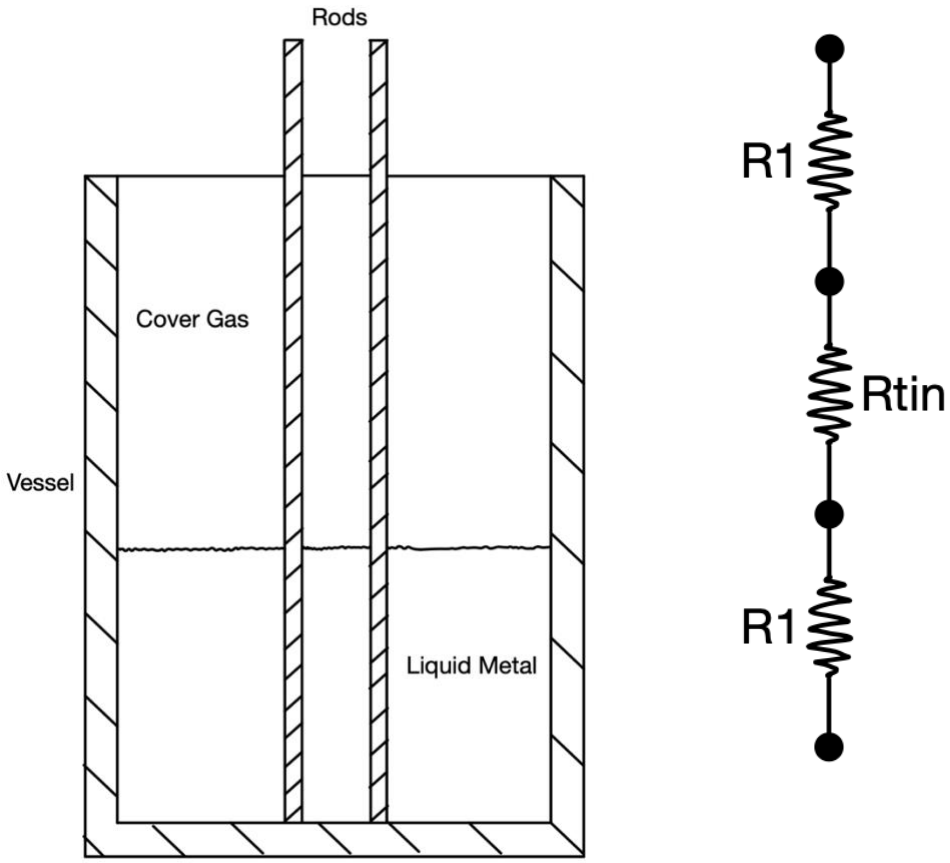

Figure 11: Simple Rod (a) Design, (b) Equivalent Circuit

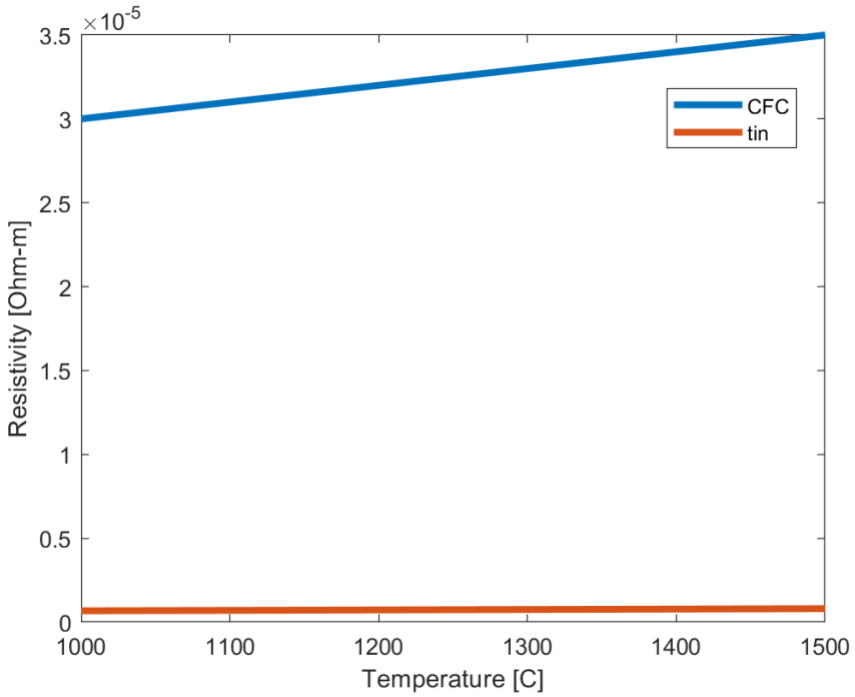

Figure 12: Resistivity of CFC and Tin

The resistivities of CFC and tin are functions of temperature, as seen by equation 16 and 17. [16] [17]

$$\rho_{CFC} = 1 \times 10^{-8} T[C] + 2 \times 10^{-5}\ \Omega m \tag{16}$$

$$\rho_{Tin} = 2.5758 \times 10^{-10} T[C] + 4.1825 \times 10^{-7}\ \Omega m \tag{17}$$

As shown by figure 12, the resistivity of CFC is orders of magnitude larger than tin across all temperatures. The total circuit resistance is a function of the two rod resistances and the tin resistance, which in turn are a function of the design geometry and the material's resistivity as seen by equations 18, 19, and 20.

$$R_1 = \rho_{CFC} \frac{4(L_{rod} - h)}{\pi D_{rod}^2}\ \Omega \tag{18}$$

$$R_{Tin} = \rho_{Tin} \frac{w}{h D_{rod}}\ \Omega \tag{19}$$

$$R_{tot} = 2R_1 + R_{Tin}\ \Omega \tag{20}$$

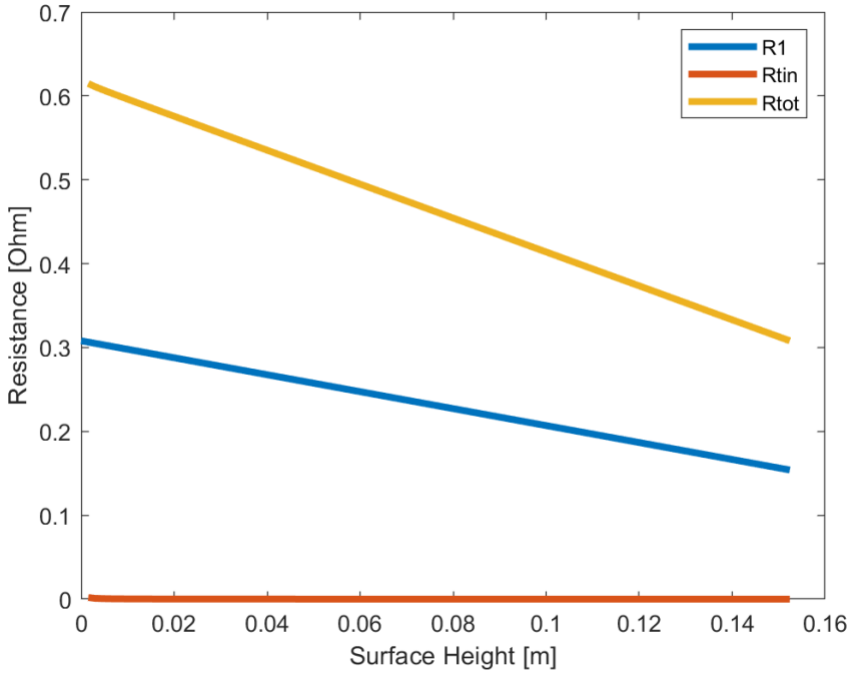

Figure 13: Simple Rod Design Resistances

Figure 13 shows that resistance varies linearly with height. The resistance of the tin is shown as negligible except perhaps at h = 0+, because a very thin layer of tin corresponds to a higher resistance. This end effect can be removed by having the rods already partially immersed in tin before the liquid level reaches the outlet orifice. Resistance can be linked back to flow rate based on these heights through equation 7, the result of which can be seen in figure 14.

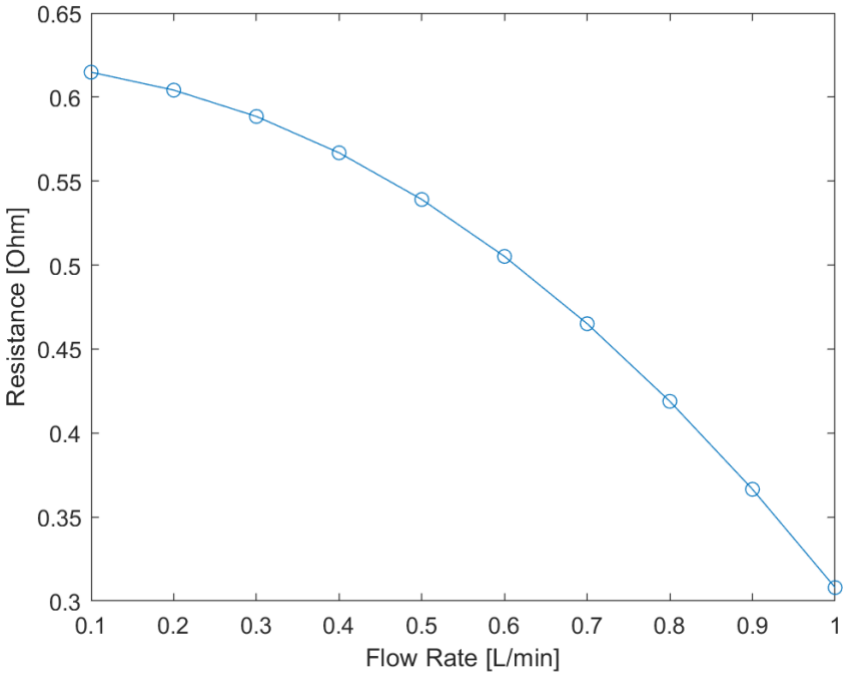

Figure 14: Simple Rod Design Calibration Curve

This resistance measurement, however, is also a function of temperature. For accurate results, a thermocouple would be required to measure temperature in the tank in order to select the correct calibration curve. As seen in figure 15, the temperature sensitivity at higher flow rates is not as significant, but at lower flow rates, fluctuations in temperature will cause large errors and cannot be ignored. For example, if the system was running at 1200 ºC and 0.2L/min, the resistance would read ~0.302 Ω. If the measurement changed to 0.306 Ω one might expect that the flow rate had dropped to 0.1L/min, but that same change in resistance measurement corresponds with a 50 ºC increase in temperature.

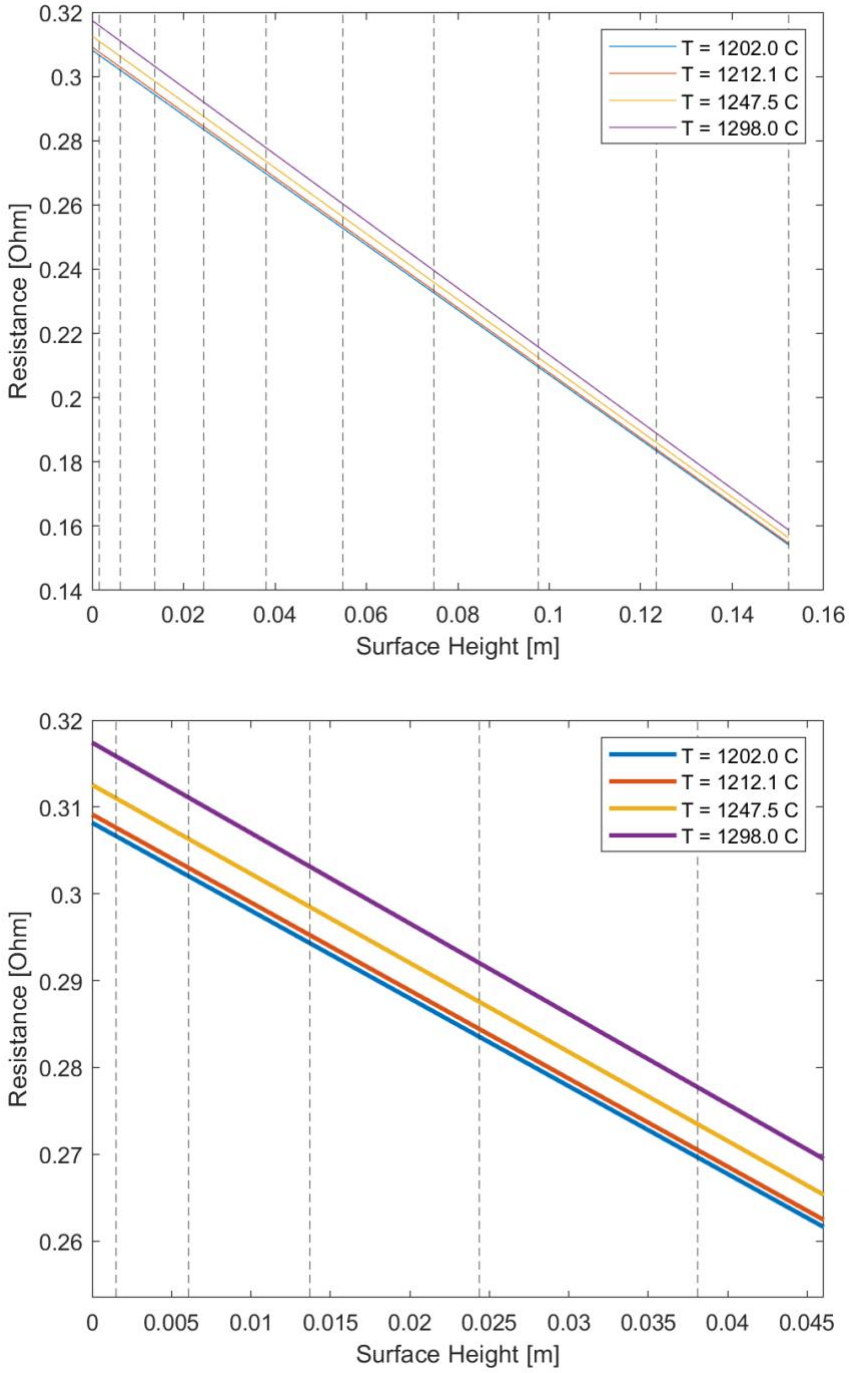

Figure 15: Simple Rod Design Temperature Dependence

6.2 Rod-Sheath Design

Temperature dependence can be innately compensated for by changing the probe design and its equivalent circuit. Specifically, temperature compensation can be achieved by creating an output that depends on a ratio of resistances. As long as those resistors are made of the same material, the ratio of their resistances will remain the same for all temperatures. This can be accomplished by the addition of a sheath around one of the CFC rods. The sheath should be made of a low resistivity material such as tungsten or have a geometry that lends itself to a low resistance. The rod inside the sheath now acts as a reference resistor. The reference rod does not contact the liquid metal and therefore its resistance does not vary with height. At high enough temperatures, everything within the tank should be at thermal equilibrium so the reference rod's temperature should match that of the active rod. The reference rod should be electrically connected to the closed bottom of the sheath but be electrically isolated everywhere else. This can be accomplished by drilling a blind hole at the bottom of the sheath for the rod to fit into and pouring in a small amount of tin or conducting paste to ensure complete electrical contact. At the top, an insulating bushing should be placed between the rod and the sheath which can be made of a high temperature ceramic such as alumina. Finally, a collar should be fit around the top of the sheath to be able to bring a lead wire out of the high temperature environment.

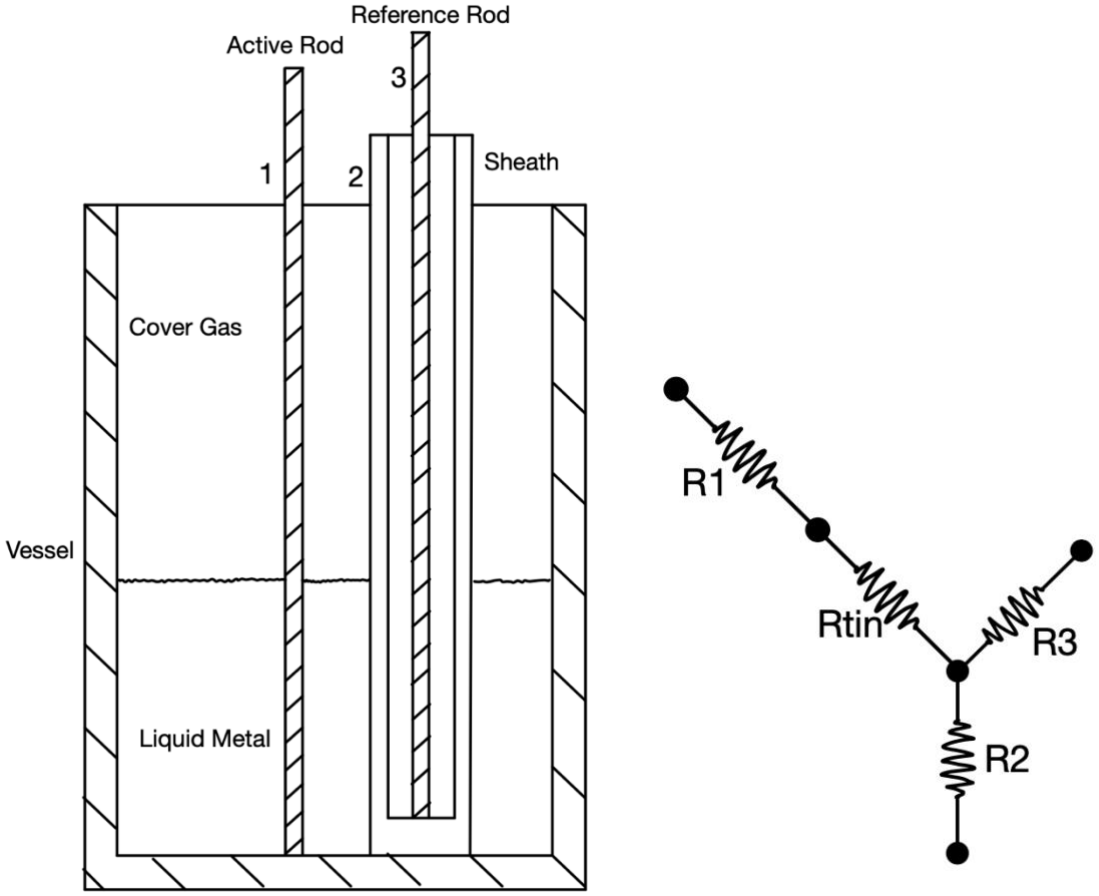

Figure 16: Rod-sheath (a) Design, (b) equivalent circuit

Nominal choices put the tungsten sheath at 1" outer diameter, 1/16" thickness, 7/8" inner diameter, and 9" length, with 1" of space between it and the active rod. The design and its equivalent circuit are shown in figure 16.

The resistivity of tungsten (W) is a function of temperature as seen by equation 21. [18]

$$\rho_W = 1.891 \times 10^{-14} T^2[C] + 2.49 \times 10^{-10} T[C] - 9.74 \times 10^{-8}\ \Omega m \quad (21)$$

As shown by figure 17, the resistivity of tungsten is on the same order of magnitude as tin across all temperatures. The reference rod resistance and the sheath resistance are a function of the design geometry and the material's resistivity as seen by equations 22 and 23.

$$R_2 = \rho_W \frac{4(L_{sheath} - h)}{\pi(OD^2_{sheath} - ID^2_{sheath})}\ \Omega \quad (22)$$

$$R_3 = \rho_{CFC} \frac{4(L_{rod})}{\pi D^2_{rod}} \quad (23)$$

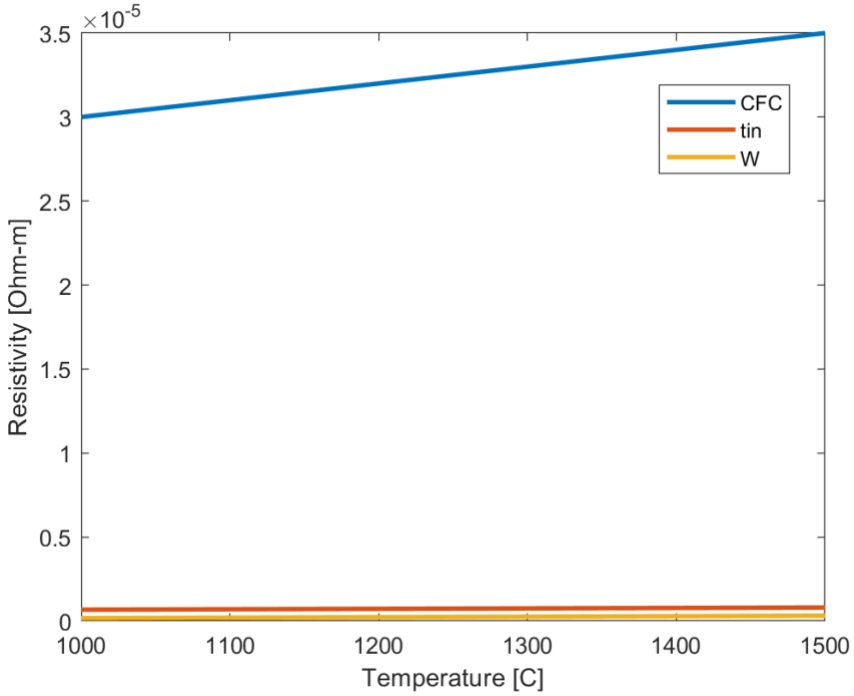

Figure 17: Resistivity of CFC, Tin, and Tungsten

Figure 18 shows that the resistance of the reference rod is constant, the resistance of the active rod varies linearly with height, and the resistances of the tin and the sheath are negligible.

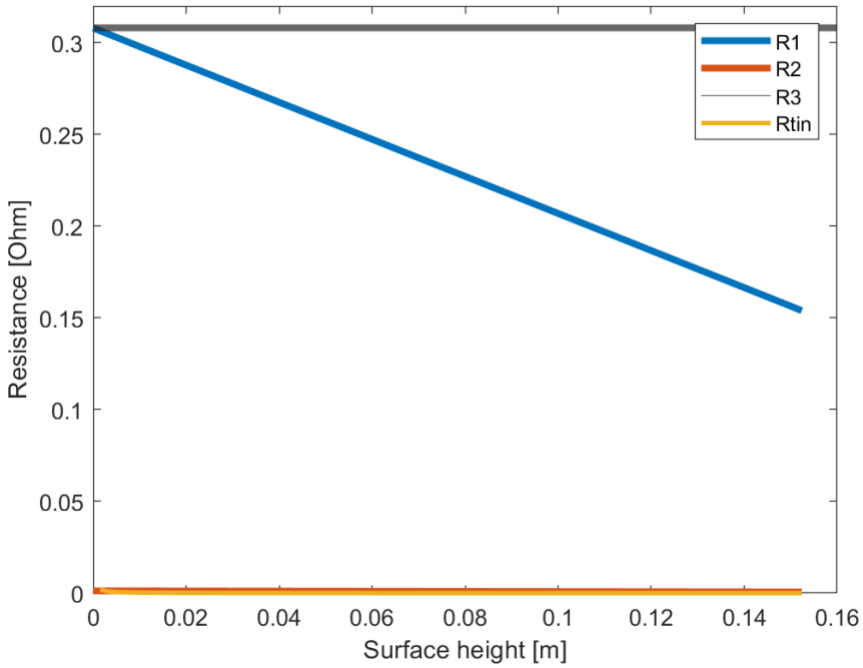

Figure 18: Rod-Sheath Design Resistances

With this setup, there are two options to create a temperature-insensitive output. The first option is to create a voltage divider as seen in figure 19. This can be done by connecting the active rod to a voltage input and connecting the reference rod to ground. In this case, the sheath acts as a lead wire that splits the two rod resistors. The potential difference between the top of the active rod and the sheath is measured as the output voltage, which follows the voltage divider rule as shown in equation 24. [19]

$$E_{out} = V_{in}\left(\frac{R_1}{R_1+R_3}\right) \tag{24}$$

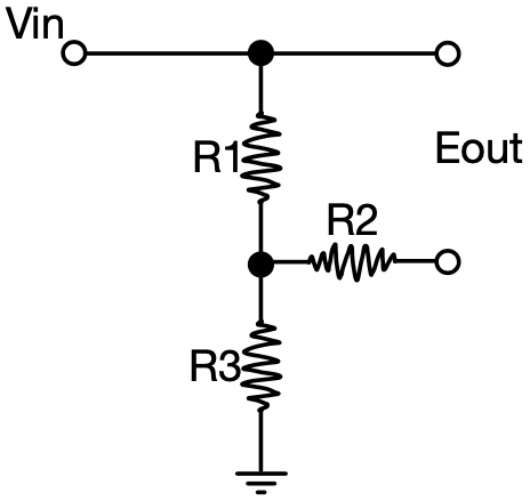

Figure 19: Rod-Sheath Voltage Divider Circuit

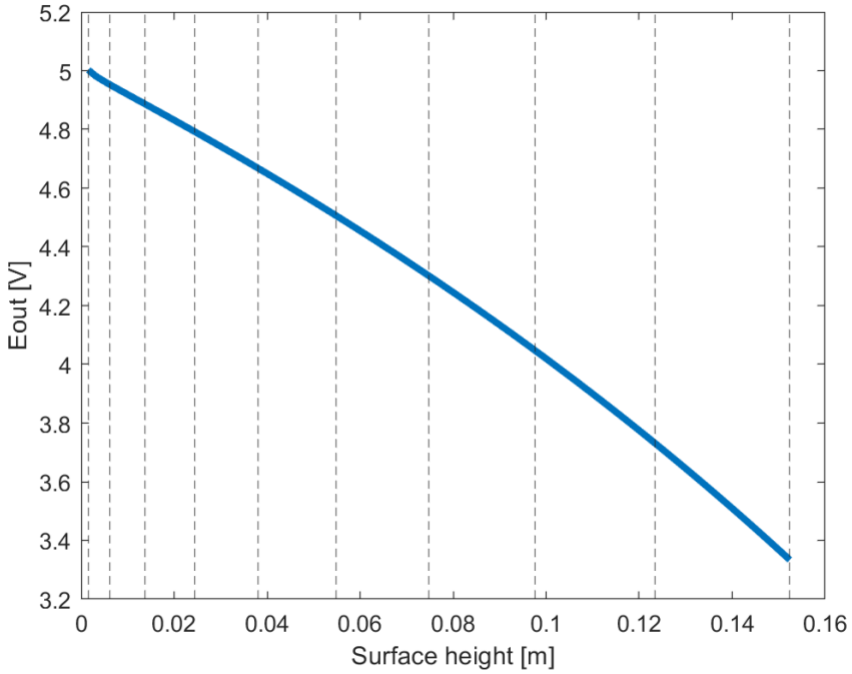

Figure 20: Rod-Sheath Design Voltage Divider Output

The resistor ratio in equation 24 cancels out the temperature dependence, but introduces non-linearity with respect to height as seen in figure 20 where Vin is 10V.

The other option is to place both rods in parallel, connecting them to a voltage input and connecting the sheath to ground. This creates a branch for each rod as seen in figure 21. By taking two measurements and computing the ratio of one branch to the other, a linear, temperature insensitive output can be achieved. This can be done by measuring the current passing through each branch as seen in equations 25, 26, and 27.

$$I_{II} = V_{in}\left(\frac{R_1+R_{Tin}}{(R_1+R_{Tin})(R_2+R_3)+R_2R_3}\right)\ [A] \tag{25}$$

$$I_I = \frac{V_{in} - I_{II}(R_2+R_3)}{R_2}\ [A] \tag{26}$$

$$Output = \frac{I_{II}}{I_I} \approx \frac{R_1}{R_3} \tag{27}$$

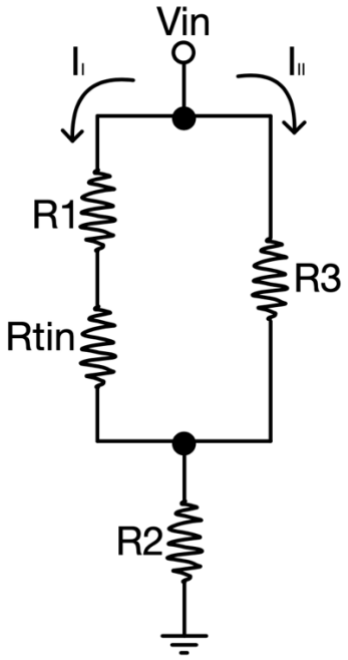

Figure 21: Rod-Sheath Design Two Branch Circuit

In order to reduce joule heating, current should be kept relatively low. If input voltage is set at 1V, current through the active rod will range from 3-7A. The branch currents and output ratio with respect to height can be seen in figures 22 and 23.

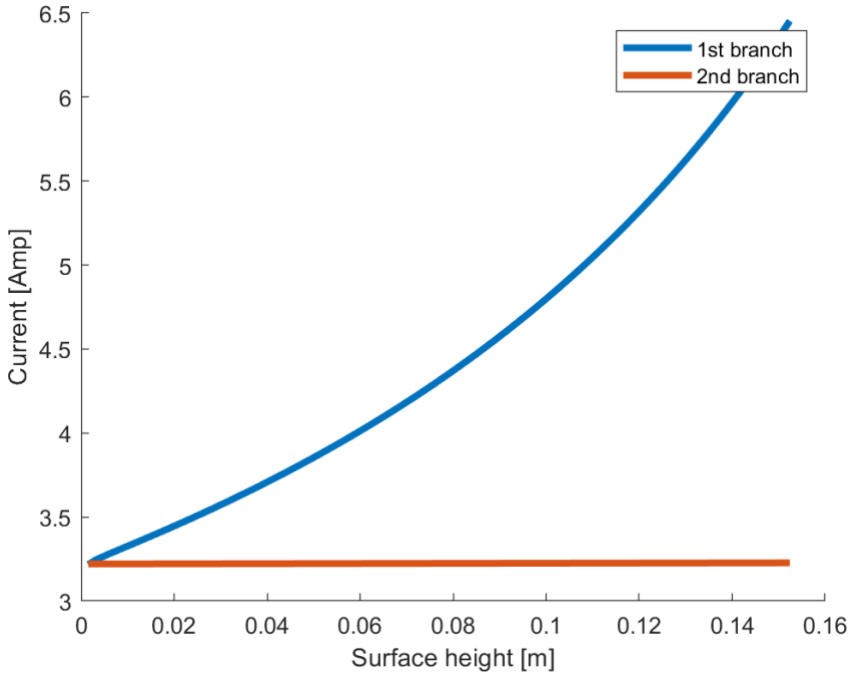

Figure 22: Rod-Sheath Design Branch Currents

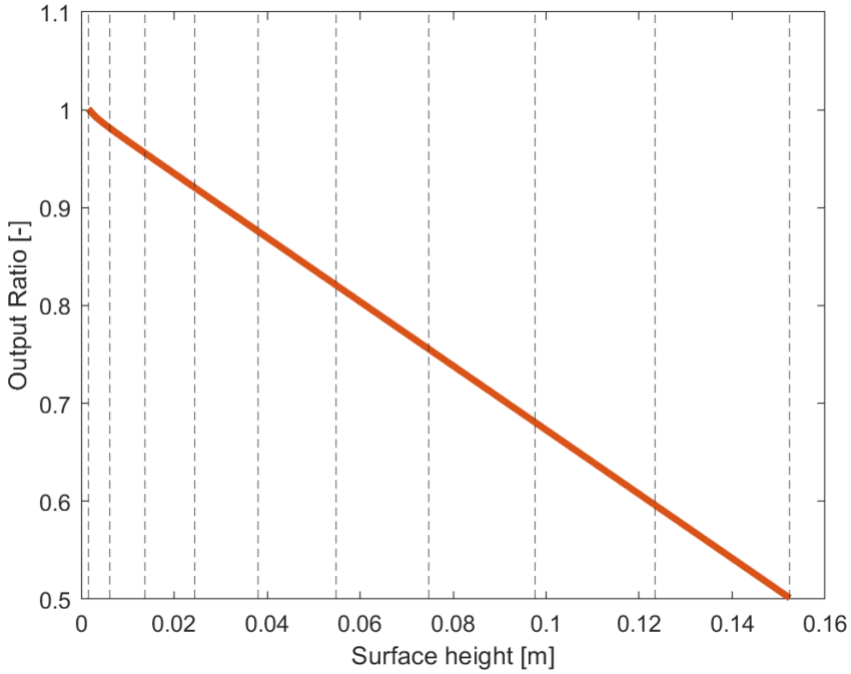

Figure 23: Rod-Sheath Design Two Branch Output

This same ratio can also be accomplished by measuring the resistance from the top of the reference rod to the sheath and the resistance from the top of the active rod to the sheath as seen in equations 28, 29, and 30.

$$R_I = R_1 + R_{Tin} + R_2 \tag{28}$$

$$R_{II} = R_3 + R_2 \tag{29}$$

$$Output = \frac{R_I}{R_{II}} = \frac{R_1 + R_{Tin} + R_2}{R_3 + R_2} \approx \frac{R_1}{R_3} \tag{30}$$

The output ratio can be linked back to flow rate through equation 7, the result of which can be seen in figure 24.

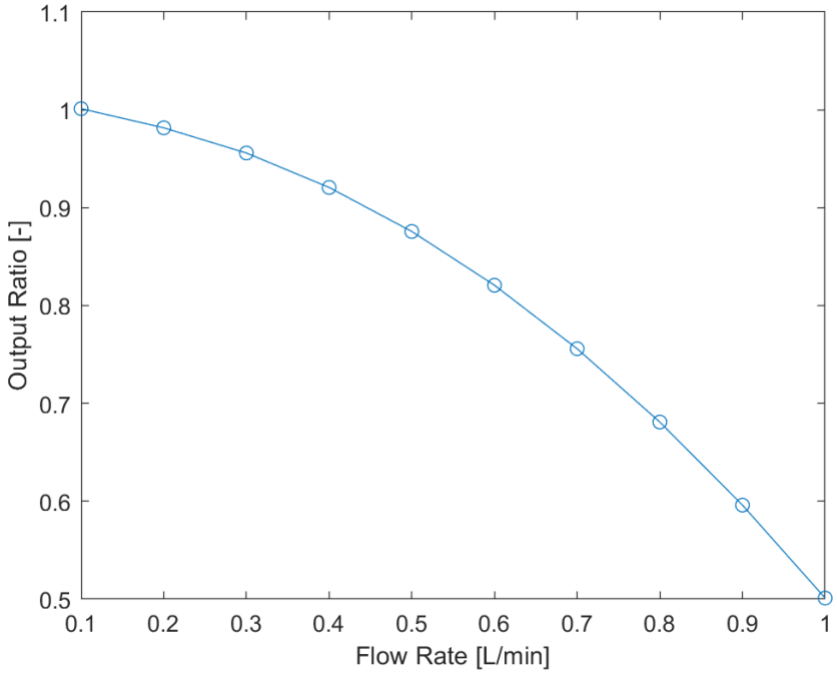

Figure 24: Rod-Sheath Design Calibration Curve

7. Resistance-Based Height Measurement Prototype and Experiments

To test the validity of the rod-sheath design, we manufactured a working prototype shown in figure 25. For the first iteration, parts from the ASE lab were incorporated as much as possible. The tank body is a bored graphite cylinder with a 4.5" outer diameter, 3" inner diameter, 6" bore depth, and 7" total height. We drilled four ¼" deep blind holes of ¼" diameter in the tank rim. For a prototype, having an entirely insulating lid is much easier than sizing multiple insulating bushings to go into a conducting lid, so lid is made from insulation brick. We drilled ¼" holes at the edges of the lid to match those in the tank rim so that pins could be dropped through to keep the lid aligned with the tank. The sheath is a closed-end graphite tube with 1.15" outer diameter, 0.75" inner diameter, 8" bore depth and 9" total height. The rods are threaded and made of carbon fiber composite (CFC) with a ¼" outer thread diameter, 0.21" inner thread diameter and a length of 12". We drilled ¼" blind holes into the inner surface of the tank and sheath bottoms so that the rods would be secured and supported at their end. A small amount of tin (or thermal conducting paste) was placed in the sheath to ensure a strong electrical connection between the bottom of the sheath and the reference rod. A piece of insulation was fit between the reference rod and the inside of the sheath to ensure electrical isolation at the top. An inlet pipe was machined from the same type of tube as the sheath by making a slot at the closed end. No outlets were necessary for this iteration as the goal was to measure liquid height without connecting it to flow rate. We cut three appropriately sized holes into the lid for the active rod, sheath, and inlet pipe to enter through.

Because electrical measuring devices will not function at extreme temperatures, the circuit must be extended out from the rods and sheath, and past the insulation layer to an area with more favorable temperatures. For the prototype, this can be accomplished for the rods by connecting them to brass threaded lead rods with brass fasteners. An electric connection can be made with the sheath by wrapping a copper collar (placed over graphite string to ensure complete contact) around the tube. The circuit can then be extended by an attached wire. Brass has a melting point ranging between 930-1000 ºC and copper has a melting point of 1084 ºC, which are suitable for the lower temperatures expected for prototype experiments, but not for a final design.

Figure 25: Rod-Sheath Height Measurement Prototype

The expected resistance R for the rods and sheath can be calculated from the material's resistivity ρ and geometry

$$R = \rho \frac{L}{A} \tag{31}$$

where L is the resistor length and A is the resistor cross-sectional area. The resistivity of CFC (see equation 16) and graphite are functions of temperature. [16]

$$\rho_C = 3.3 \times 10^{-9}\, T[C] + 6.6 \times 10^{-6}\, \Omega m \tag{32}$$

Table 1 lists the expected resistances for room temperature (25 ºC) and experimental temperature (300 ºC). The measured value at room temperature for the rod was 0.292 Ω.

Table 1: Prototype Rod and Sheath Expected Resistance

	T = 25 ºC	T = 300º C
Rod	0.2762 Ω	0.3137 Ω
Sheath	0.0040 Ω	0.0046 Ω

Initial tests were performed with water at various heights, however, no change in resistance occurred as water does not have a high enough conductivity to shunt the rod. This test was repeated with thermal paste liquid with the same lack of results. Other potential alternatives to tin for use in experiments are shown in table 2.

Table 2: Conducting Fluids [20 – 31]

Material	Melting Temperature (ºC)	Conductivity (S/m)	Safety
Tin	232	9.17e6	Oxidizes
Gallium	29.76	7.1e6	Corrosive, Irritant
Indium	156.6	12e6	Flammable, Irritant, Health Hazard
Galinstan	-19	3.46e6	
Water	0	0.05	
Salt Water	-1.332	4.5-5.5	
Citric Acid (20% by wt.)	153	0.79	Irritant
Hydrochloric Acid (HCl) (19% by wt.)	-114.2	85	Corrosive, Acute Toxic
Nitric Acid (HNO_3) (29% by wt.)	-41.6	86.5	Oxidizer, Corrosive, Acute Toxic
Sulfuric Acid (H_2SO_4) (30% by wt.)	10	82.5	Corrosive
Mercury	-38.86	1.02e6	Acute Toxic, Health Hazard, Environmental Hazard
Phosphorus	44	10e6	
Potassium	63.3	13.9e6	Flammable, Corrosive
Selenium	217	8.33e6	Acute Toxic, Health Hazard
Sodium	97.83	21e6	Flammable, Corrosive
Solder	215	6.67e6	
Graphite	3500	1.25-3e5	
Brass	930-1000	14-16.95e6	
Copper	1084	5.96e7	

7.1 Tin Experiment

The experimental procedure relies on known amounts of tin being incrementally added to the tank in order to determine the relationship between resistance and liquid height. The simplest way to do this is by weighing an amount of tin before adding it to the tank, using the density of tin and the tank geometry to determine the expected increase in liquid height. The density of tin d_{Tin} is a function of temperature

$$d_{tin} = 7374.7 - 676.5 \times 10^{-3}\, T[K]\, kg/m^3 \quad (33)$$

therefore, the expected density at experimental temperature (300ºC) is $6.987*10^3$ kg/m^3. [32]

In order to produce and sustain this temperature, the tank is placed within a resistive pipe heater paired with a temperature control box and surrounded with insulation. While the experiment can be run in air, the tin will oxidize, forming a tin oxide crust which has the potential to disrupt the experiment and its results. This can be avoided by running the experiment in the ASE lab's vacuum chamber using Argon as the cover gas. In this case, wires must be connected to the built-in electrical feedthroughs in order to reach the measuring device. The use of the vacuum chamber complicates the process of adding set amounts of tin to the tank. One method would be to completely reset the chamber between each new height measurement. While this allows for the easiest addition of new tin, it greatly increases the time it will take to run experiments. The other option is to set up units of tin near the tank so that they may be easily added in by hand using a glove box in the chamber side.

We ran the experiment in air for three different heights, one near empty, one near the middle, and one near full. Specifically, we ran the experiment for three tin masses (0.539 kg, 1.887 kg, and 3.505 kg) which corresponded to a surface height of about 2 cm, 7 cm, and 13 cm respectively. The resulting resistance measurements successfully followed the trend of our model, as seen in figure 26. Differences between the experimental results and the model could be caused by a variety of things. For one, the resistivities used for CFC and carbon in the model are most likely underestimates of the true values. Furthermore, the resistances of the extra rods and wires to bring the circuit out to the measuring device are non-negligible and contribute to a higher measured value than expected. The relationship between the height of the tin and the ratio of the two resistance measurements is shown in figure 27. These results show that the Rod-Sheath design and its resistance measurements can successfully be used to determine surface height.

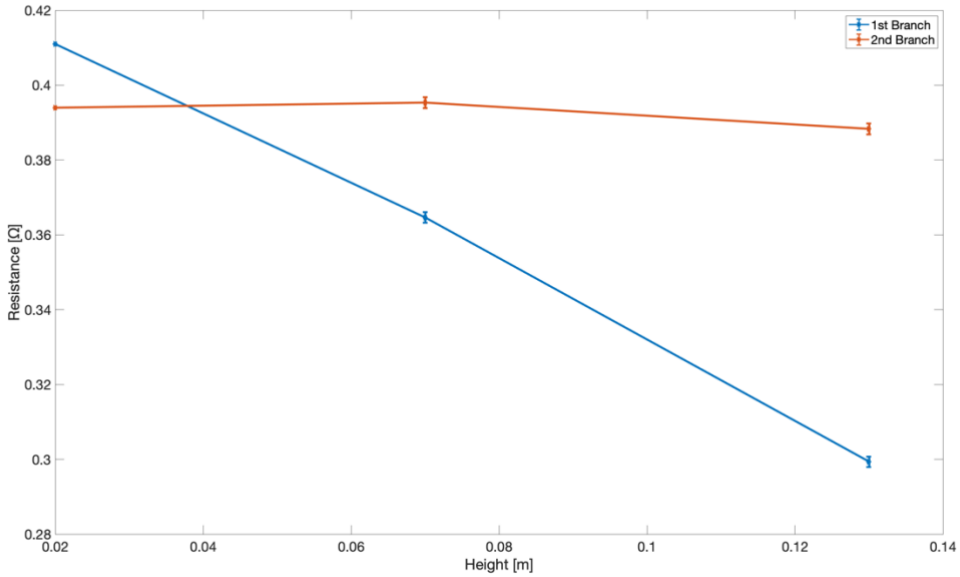

Figure 26: Prototype Measured Resistances

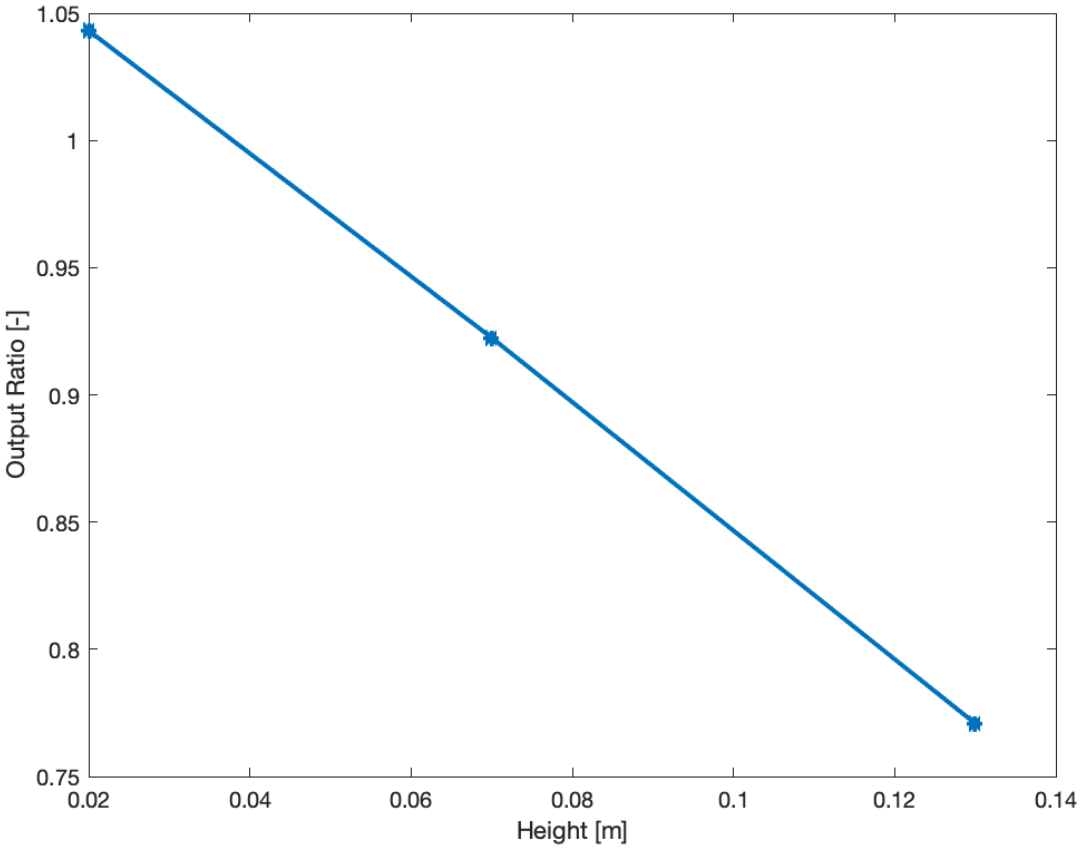

Figure 27: Prototype Experiment Output

Now that this first trial validated the proof of concept, small increments of heights can be measured to determine the resolution of the device. For the sake of robustness, this experiment should be repeated at other temperatures. While the nature of the rod-sheath design removes temperature sensitivity, other factors affected by temperature such as wetting could have a meaningful effect on the output.

8. Future Work

To better understand the flow meter's expected behavior in the actual methane pyrolysis system, the above experiment should be run for temperatures around 1200 ºC. The experiment could even be run at upwards of 2000 ºC in order to test the behavior for the purpose of other potential applications that operate at even higher temperatures. Such temperatures, however, would surpass the melting point of brass and copper, requiring the current prototype to be modified. Table 3 shows various metals that could be used to replace the fasteners and lead rods, and the tube collar and wire.

Table 3: Metal Melting Points [23]

Material	Melting Temperature (ºC)
Brass	930-1000
Copper	1084
Manganese	1244
Beryllium	1285
Monel	1300-1350
Inconel	1390-1425
Silicon	1411
Steel	1425-1540
Nickel	1453
Wrought Iron	1482-1593
Cobalt	1495
Palladium	1555
Titanium	1670
Thorium	1750
Platinum	1770
Zirconium	1854
Chromium	1860
Vanadium	1900
Rhodium	1965
Iridium	2450
Niobium (Columbium)	2470
Ruthenium	2482
Molybdenum	2620
Tantalum	2980
Osmium	3025
Rhenium	3186
Tungsten	3400

Once the current prototype proves the reliability of the sheath-rod design in measuring surface height, the next step is to test its ability to measure flow rate. While the current prototype tank could be merely modified with outlets, its dimensions are not congruent with use as a flow meter. Specifically, the 3" inner diameter and 6" height result in an equilibrium response time far greater than 60 seconds for extreme changes in flow rate. Therefore, a new tank should be used with a tank inner diameter closer to 2 or 2.5 inches. With this new tank, for there to be enough room between the rod, sheath, inlet pipe, and walls to ensure electrical isolation, it may be worth using smaller tubes for the sheath and inlet pipe with outer diameters closer to ½".

9. Summary

Through this research, we have developed a viable design for a flow meter able to measure the 1200 ºC liquid tin pumped through the ASE Research Group's methane pyrolysis system. Such a design has applications in a wide variety of energy technologies and industrial processes. The novel rod-sheath design offers accurate flow rate measurement regardless of temperature changes, with sufficient resolution provided by a range characterized by a minimum measured value that is half that of the maximum. Due to the non-linearity of Torricelli's law, measurements will be most accurate and differentiable at higher flow rates.

REFERENCES

1. Atomic Simulation & Energy Research Group, accessed May 6, 2022. https://ase.mit.edu/
2. Chemistry Explained: Foundations and Applications, accessed May 6, 2022. http://www.chemistryexplained.com/elements/T-Z/Tin.html
3. Argyropoulos, Stavros A., 2001, Measuring velocity in high-temperature liquid metals: a review. Scandinavian Journal of Metallurgy 2000; 30: 273-285 .
4. Malcherek, Andreas, 2016, History of the Torricelli Principle and a New Outflow Theory. Journal of Hydraulic Engineering 142(11).
5. Lienhard (V), J. H., Lienhard (IV), J. H., 1984, Velocity Coefficients for Free Jets From Sharp-Edged Orifices, Journal of Fluids Engineering 106(1).
6. Amy, Caleb Amos, 2017, Liquid Metal Pumps for Enabling Heat Transfer at Extreme Temperatures, The Georgia Institute of Technology.
7. DeAngelis, Alfred, 2016, Analysis and Design of a High Temperature Liquid Metal Solar Thermal Receiver, The Georgia Institute of Technology.
8. How Stuff Works: How Digital Scales Work, accessed May 6, 2022. https://electronics.howstuffworks.com/gadgets/fitness/digital-scale.htm
9. Slocomb, H. W., 1967, Liquid Metal Level Measurement (Sodium) State-of-the-Art-Study, Liquid Metal Engineering Center Operated for the U.S. Atomic Energy Commission.
10. Reshma, R., Ramachandraiah, U., Devabalaji, K. R., and Sitharthan, R., 2020, Liquid Metal Level Measurement Techniques, IOP Conference Series: Materials Science and Engineering 937 012027.
11. Sehgal, Bal Raj, 2012, Nuclear Safety in Light Water Reactors: Severe Accident Phenomenology
12. Briggs, N. H., et al., 1968, Temperature-Gradient-Insensitive Resistance-Type Liquid Metal Level Detector. United States, US3369401A.
13. Kidd, Martin L. 2012, Watch Out for Those Thermoelectric Voltages! The International Journal of Metrology.
14. Cambillard, E., Lions, N., 1966, Instrumentation des Circuits de Sodium, Proceedings of a Symposium on Alkali Metal Coolants, Vienna, pg 617-629.
15. Affel, R.G., Burger, G.H., Pidgeon, R.E., 1960, Level Transducers for Liquid Metals, Oak Ridge National Laboratory.
16. Okada, Masaki, et al., 2017, Review on the High-Temperature Resistance of Graphite in Inert Atmospheres, Carbon vol 116 pg 737-743.
17. Gasser, J. G., et al., 1985, Temperature Dependence of the Liquid Tin Resistivity, phys. stat. sol. (b) 128, 789.
18. The Physics Factbook: Resistivity of Tungsten, accessed May 6, 2022. https://hypertextbook.com/facts/2004/DeannaStewart.shtml
19. Oxford University Press, 2009, A Dictionary of Physics (6 ed.)
20. The Engineering ToolBox: Electrical Conductivity – Elements and other Materials, accessed May 6, 2022. https://www.engineeringtoolbox.com/conductors-d_1381.html
21. The Engineering ToolBox: Resistivity and Conductivity – Temperature Coefficients Common Materials, accessed May 6, 2022. https://www.engineeringtoolbox.com/resistivity-conductivity-d_418.html

22. The Engineering ToolBox: Melting and Boiling Temperatures – Evaporation and Melting Heats common Materials, accessed May 6, 2022. https://www.engineeringtoolbox.com/resistivity-conductivity-d_418.html
23. The Engineering ToolBox: Metal and Alloys – Melting Temperatures, accessed May 6, 2022. https://www.engineeringtoolbox.com/melting-temperature-metals-d_860.html
24. ThoughtCo: Table of Electrical Resistivity and Conductivity, accessed May 6, 2022. https://www.thoughtco.com/table-of-electrical-resistivity-conductivity-608499
25. Periodic Table: Elements, accessed May 6, 2022. https://periodictable.com/Elements/
26. Surmann, P., Zeyat, H., 2005, Voltammetric Analysis Using a Self-Renewable Non-Mercury Electrode, Analytical and Bioanalytical Chemistry 383, 1009-1013.
27. Karcher, Ch., et al., 2003, Experimental Investigations of Electromagnetic Instabilities of Free Surfaces in a Liquid Metal Drop, International Scientific Colloquium: Modelling for Electromagnetic Processing.
28. Britannica: Seawater, accessed May 6, 2022. https://www.britannica.com/science/seawater/Thermal-properties
29. Gilson Engineering Sales, Inc.: Index of Electrolytes, accessed May 6, 2022. https://www.gilsoneng.com/reference/conductivity%20acids.pdf
30. Material Properties: What is Electrical Resisitivity of Soft Solder – 60-40 Solder – Definition, accessed May 6, 2022. https://material-properties.org/what-is-electrical-resisitivity-of-soft-solder-60-40-solder-definition/
31. PubChem: Explore Chemistry, accessed May 6, 2022. https://pubchem.ncbi.nlm.nih.gov/
32. Alchagirov, B. B., Chochaeva, A. M., 2000, Temperature Dependence of the Density of Liquid Tin, Thermophysical Properties of Materials: High Temperature 38, 44-48